

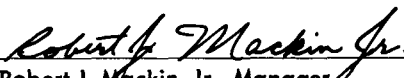
NATIONAL AERONAUTICS AND SPACE ADMINISTRATION

Technical Memorandum No. 33-283

*Fluid Systems Design Concept for a Large
Gas-Cooled Fission-Electric Cell Reactor
Space Power Plant*

D. J. Mokski

Approved by:


Robert J. Mackin, Jr., Manager
Physics Section

JET PROPULSION LABORATORY
CALIFORNIA INSTITUTE OF TECHNOLOGY
PASADENA, CALIFORNIA

February 1, 1967

Copyright © 1967
Jet Propulsion Laboratory
California Institute of Technology
Prepared Under Contract No. NAS 7-100
National Aeronautics & Space Administration

CONTENTS

I. Introduction	1
II. Temperature Distributions, Pressure Drop, and Pumping Power for a Gas-Cooled Fission-Electric Cell Reactor	3
A. Reactor Temperature Distributions	5
1. Fluid Stagnation Temperature and Wall Temperature	5
2. Cathode and Anode Surface Temperatures	6
B. Reactor Pressure Drop and Pumping Power	9
1. Pressure Drop	9
2. Pumping Power	13
III. Temperature Distribution, Pressure Drop, and Pumping Power for the Single Phase Radiator	18
A. Radiator Temperature Distribution	18
B. Radiator Size	20
C. Radiator Pressure Drop and Pumping Power	22
IV. Suggested Plant Design Concept	25
V. Weight Estimate — Gas-Cycle Components	28
A. Reactor Core Weight	28
B. Reflector Weight	28
C. Spherical Pressure Vessels	28
D. Reactor Inlet Manifold and Manifold Feeder Pipes	28
E. Radiator Area	28
F. Radiator Weight	29
1. Manifold Weight	29
2. Radiator Tube Weight	29
3. Involute Reflector Weight	29
4. Gas Cycle Radiator Total Weight	29
G. Compressor and Compressor Driver Weight	30
H. Weight Totals—Fission-Electric Cell Reactor Gas Cycle	30
VI. Weight Estimate — Driver-Cycle Components	30
A. Discussion	30
B. Driver Cycle Weight Estimates — Potassium Vapor Cycle	31
1. ORNL Drawings	31
2. Reactor	31
3. Turbines and Pumps	32
4. Generator	32
5. Miscellaneous Weight Items	32
6. Weight Totals — Driver Plant	32

CONTENTS (Cont'd)

VII. Weight Summary	33
A. Weight Summary for 5% Conversion Efficiency	33
B. Effect of Improved Fission-Electric Cell Conversion Efficiency	33
VIII. Conclusions	34
Appendix: Reactor Pressure Drop	35
Nomenclature	39
References	39
Bibliography	41

TABLES

1. Various cell geometries considered in this study	4
2. Heat transfer information for cell geometries tabulated in Table 1	4
3. Values of the non-dimensional parameter $4f L/D (1/P_r)^{0.6}$ for the L/D values considered in this study	6
4. Tabulation of parameters \mathcal{D}_1 and \mathcal{D}_2 in terms of bulk inlet and outlet temperatures, for use in Eq. (14 and 17)	10
5. Results of reactor pressure drop calculations, hydrogen, $D_w = \text{constant} = 0.50$ in.	11
6. Results of reactor pressure drop calculations, helium, $D_w = \text{constant} = 0.50$ in.	12
7. Results of reactor pressure drop calculations, hydrogen, $p_{o2} = \text{constant} = 250$ psia	12
8. Results of reactor pressure drop calculations, helium, $p_{o2} = \text{constant} = 250$ psia	13
9. Radiator thermal parametric analysis results	21
10. Radiator hydraulic parametric analysis results	23
11. Weight totals, fission-electric reactor gas cycle	30
12. Weight totals, driver plant	32
13. Comparison, gas cycle vs driver cycle	33
A-1. Evaluation of the parameters \mathcal{D}_1 and \mathcal{D}_2	37

FIGURES

1. Fission-electric cell geometry and nomenclature	3
2. Fission-electric reactor showing assumed heat-load distribution	3
3. Fission-electric cell conversion efficiencies vs fuel-layer thickness expressed as a fraction of mean fission fragment range for various anode-cathode diameter ratios	4
4. Reactor tube showing parabolic distribution of heat input and nomenclature	5
5. Coolant stagnation temperature variation with distance into the reactor coolant channel for various values of $T_{o2} - T_{o1}$ (parabolic distribution of heat input)	5
6. Coolant channel wall temperature variation for parabolic distribution of heat input and various values of $4f(L/D)(1/P_r)^{0.6}$	6
7. Coolant channel wall temperature variation for parabolic distribution of heat input with conditions listed	7
8. Fission-electric cell cross section	7
9. Reactor pumping power parametric study at 4000°R, with H ₂	14
10. Reactor pumping power parametric study at 3500°R, with H ₂	15
11. Reactor pumping power parametric study at 3000°R, with H ₂	15
12. Reactor pumping power parametric study at 4000°R, with He	16
13. Reactor pumping power parametric study at 3500°R, with He	16
14. Reactor pumping power parametric study at 3000°R, with He	16
15. Reactor pumping power parametric study at 4000°R and 250 psia, with H ₂	17
16. Reactor pumping power parametric study at 3500°R and 250 psia, with H ₂	17
17. Reactor pumping power parametric study at 3000°R and 250 psia, with H ₂	17
18. Reactor pumping power parametric study at 4000°R and 250 psia, with He	17
19. Reactor pumping power parametric study at 3500°R and 250 psia, with He	18
20. Reactor pumping power parametric study at 3000°R and 250 psia, with He	18
21. Point-by-point thermal analysis of a radiator tube	19
22. Radiator tube temperature distributions	21
23. Radiator relative size variation vs mass flux (ρV)	22
24. Radiator relative weight variation vs mass flux (ρV)	22
25. Relationship between length/diameter ratio (L/R) and mass flux (ρV), radiator tubes	22
26. Radiator pumping power as a function of mass flux (ρV), $p_{o1} = 480$ psia	24
27. Radiator pumping power as a function of mass flux (ρV), $p_{o1} = 380$ psia	24
28. Radiator pumping power as a function of mass flux (ρV), $p_{o1} = 280$ psia	24
29. Summary of radiator parametric analysis	24
30. Gas-cooled fission-electric reactor and radiator concept	26
31. The involute reflector	27

ABSTRACT

The possibility of using a gas to transport waste heat from a large fission-electric cell reactor directly to a radiator is examined in order to obtain an estimate of : 1) the pumping power that would be required for such a system, 2) the size and weight of the reactor, radiator and other major components, and 3) temperature distributions in the core and other parts of the system. Also, since recent calculations have shown that long core endurance (10,000 hr) might be achieved with the aid of highly loaded driver fuel modules, a separate coolant circuit is assumed for removing heat energy from this portion of the core and converting it to electrical power for pumping and auxiliary power by means of a Rankine cycle. This auxiliary power supply would employ turbine-driven alternators and a condensing-radiator operating at a considerably lower temperature than the primary radiator mentioned above, but with only a fraction of the heat load carried by the coolant loop for the fission-electric cell portion. The sizes and weights of the major components of the auxiliary power system are also estimated. An overall specific weight of about 6.9 to 13.0 lb/kwe, not including shields, is obtained depending on the conversion efficiency: the higher weight corresponds to 5% conversion efficiency; the lower, to 10%. As might be expected, the radiator is found to be the largest and heaviest single component. However, due to the fact that the fission-electric cell power conversion concept does not require a temperature differential between anode and cathode in order to produce power, the advantage in being able to radiate at a higher temperature is found to result in a potential reduction in radiator area of from 50 to 80% (depending on efficiency) as compared with that required for a comparable plant operating on a thermodynamic power-conversion cycle.

I. INTRODUCTION

From the standpoint of the waste-heat disposal problem, the major advantage of a fission-electric cell reactor over other direct conversion systems and all power conversion systems operating on thermodynamic cycles is that the fission-electric cell energy conversion mechanism does not require a temperature differential for its operation. Unlike thermionic and thermoelectric units, the cathode and anode of a fission-electric cell may be operated at the same temperature, which can be set as high as material limitations permit. This advantage, in terms of reduced radiator size and weight, can readily be appreciated when considering a thermodynamic power-conversion cycle which operates between 2000°F peak and 1200°F sink (radiator) temperature. If the turbine could be replaced by a direct conversion device which did not require a temperature differential to function, the radiator could then operate at an effective temperature of about 2000°F and, owing to the T^4 dependence of radiative heat transfer, the radiator surface area could be reduced, for the same radiator heat load, by a factor of $(2460/1660)^4 \approx 5$. Such an improvement would result in a drastic reduction in radiator, and therefore plant, weight at fixed power level; and, because of the reduced surface area, would also offer a greatly reduced probability of meteoroid penetration. Similarly, utilizing multiple coolant loops and independent radiator sections, larger power plant outputs should be possible for a given size and weight plant without reducing reliability.

The reactor considered here would be a thermal reactor 10 ft in diameter and 10 ft in length, and would have as its fuel elements, fission-electric cells of cylindrical geometry. This study assumes an operating voltage of 10⁶v and 1-cm vacuum gaps separating the inner electrodes (cathodes), which are plated with the fuel-bearing material, from the outer electrodes (fission-fragment collectors or anodes). The moderator volume to total volume ratio is set at 0.5. The total reactor power is set at 500 Mw. The desired minimum power level of 25 Mwe would then be achieved for a conversion efficiency of 5%.

This reactor configuration represents a scale-up of a 20-Mw (1-Mwe) reactor roughly 5 ft in diameter and 5 ft in length, for which reactor physics calculations have been carried out, Ref. 1 and 2. The 20-Mw case assumed a power density of about 0.33 Mw/ft³. A power density of 0.64 Mw/ft³ has been assumed for the larger core. Since the fission-electric cell reactor would consist of about 50% void volume, the increased power density would be equivalent to about 1.28 Mw/ft³ in a conven-

tional gas-cooled power reactor, and this is consistent with current gas-cooled power reactor practice.

It should be mentioned here that certain fundamental obstacles to successful fission-electric cell operation have not yet been surmounted. The most difficult task is to achieve the required voltage (10⁶ v) over a 1-cm vacuum gap.

There are several reasons for considering a gaseous coolant for the fission-electric cell reactor:

1. The fission-electric cell reactor is inherently a low-power density reactor. This is largely due to a combination of the high void volume and the very thin fuel layer (one fission-fragment range or less) required for high conversion efficiencies, Ref. 1.
2. Significantly higher temperatures appear ultimately possible with gas-cooled reactors than with liquid metal-cooled reactors. This judgment is based on: 1) recent literature on the subject, e.g., Ref. 3 and 4, in which gas outlet temperature as high as 4700°R and higher are contemplated; 2) consideration of projects in being such as the Ultra High Temperature Reactor Experiment (helium/graphite system, T_{out} 2860°R); 3) continuing progress in the area of hydrogen cooled nuclear rocket technology; and 4) individual experiments, such as Ref. 5, in which various measurements were made on hydrogen gas at approximately 5000°R flowing in tungsten tubes and at Reynolds numbers on the order of 10⁵. The apparent higher temperature potential available with gaseous coolants is partially offset by the larger temperature drops to be expected across heat transfer surfaces cooled by a gas. However, despite large temperature drops expected with a gaseous coolant and with no temperature differential required for energy conversion, the effective temperature of a radiator for a gaseous coolant such as hydrogen or helium could exceed by 1000°R the radiator temperatures presently being considered for systems employing metal or liquid metal vapor coolants.
3. The use of gaseous coolant avoids many of the problems associated with two-phase condenser-radiators and corrosion by liquid metals, e.g., Ref. 6 and 7.
4. Gas-cooled reactors and gas cycle turbo-machinery have been notably trouble-free over years of accumulated operation, whereas alkali metal systems have yet to demonstrate a long-life performance.

Some gas turbines, notably Escher Wyss installations, have operated for longer than 10,000 hr. of almost continuous operation (90% or greater load factor) with little or no maintenance at turbine inlet temperatures of about 1500°F. For the design concept proposed here it would be required to operate a low $\Delta p/p$ compressor rather than a turbine at about the same temperature for 10,000 hr.

5. The effect of thick meteoroid armor permits high radiator gas pressures without further weight penalties. The increased operating pressure in turn improves the heat transfer characteristics of the gas and reduces pumping power requirements.

With regard to Items 3 and 4 above, attention should be called to the redesigned SNAP 8: 35-50 kwe NaK cooled reactor, Hg turbine loop NaK radiator, Ref. 8. In the referenced article, major changes have been made in the system design that will cause total weight to be "several times" heavier than the original target of 1400 lb, in an effort to improve chances of meeting the 10,000-hr reliability target. Ref. 8 also states that the major change is the addition of a third liquid metal loop to separate the condenser and radiator functions, to "get better control over the liquid interface in the condenser" since in the old arrangement "there was the danger that accelerations in flight might disrupt the liquid interface at some point and allow a slug of vapor to reach the pump. Separated from the radiator, the condenser can now be designed more compactly and with shorter tubes to minimize the possibility of vapor entrainment." A second important change eliminates the "troublesome mercury-lubricated sleeve bearings that had been planned for the turbine and alternator and substitutes conventional ball bearings lubricated and cooled with an organic" which "necessitates the addition of a second radiator" to cool the organic.¹

¹In contrast with the apparent liquid metal bearing problem, it is pointed out in Ref. 9 that "use of gas bearing might lead to a system with almost indefinitely long reliability."

With regard to the meteoroid armor question, the observation of Item 5 above could be a significant factor in favor of the type of radiator proposed in this report. It was found that for minimum weight the radiator tubes should be as small in diameter as practicable, so a 0.25-in. ID tube was selected. To minimize pumping power on the other hand, it was found that gas pressures as high as 500 psi should be considered. The combination of high gas pressures and high temperature at the tube inlet requires a tube wall thickness of about 0.11 in. and consists of a combined tungsten-and-graphite tube to keep the tube wall stresses well under 1000 psi and well within the long time (10,000 hr) tensile creep strength limitations at peak tube-wall temperatures² of about 3500°R.

It is felt that a thick tube such as this might provide sufficient armor against meteoroid penetration without additional weight penalty, although the problem has not been investigated in detail. The SNAP 2 radiator specifications (Ref. 10) make an interesting comparison:

Tube dimensions (steel)	0.366 in. OD 0.273 in. ID
Shell thickness (aluminum)	0.028 in.

Despite the considerably lower operating pressure of the SNAP 2 radiator, ≈ 15 psia or less, the combined tube and shell thickness for meteoroid protection is only 30% less than the high-temperature high-pressure gas radiator tubes considered in this report. The steel radiator tubes for SNAP 2 weigh about 0.14 lb/ft as compared with 0.13 lb/ft for the combined tungsten-graphite tubes assumed here.³

²Thin tungsten tube liner was assumed for low-temperature strength and was to function as a gas diffusion barrier.

³10-mil tungsten, 0.10-in. graphite 0.25-in. ID; specific gravity of steel is 8, graphite 1.65, tungsten 20.

II. TEMPERATURE DISTRIBUTIONS, PRESSURE DROP AND PUMPING POWER FOR A GAS-COOLED FISSION-ELECTRIC CELL REACTOR

Cylindrical geometry is assumed for the fission-electric cells, with the cells arranged in a triangular lattice as shown in Fig. 1.

To account for the non-uniform distribution of fission heat generation, the flux shapes shown in Fig. 2 were used. With the assumption of a parabolic axial distribution of heat flux, the variation of coolant stagnation temperature and tube wall temperature along the length of the tube can be calculated in a straightforward manner for specified values of T_{in} and T_{out} as is shown in Section II-A.

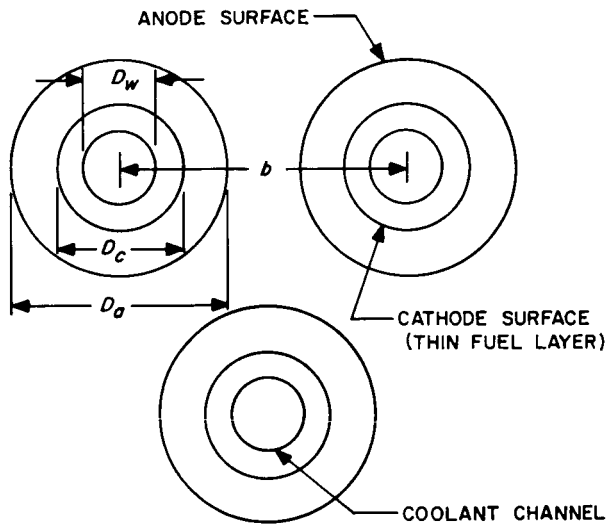


Fig. 1. Fission-electric cell geometry and nomenclature

For purposes of calculating pressure drops and pumping power, some additional assumptions are required. First of all, a reasonable estimate of the peak to average variation of radial flux had to be obtained. It was assumed that the radial distribution of thermal neutron flux, and therefore heat flux, is adequately represented by the Bessel function $J_0(r)$ with the flux vanishing at the extended boundary of the core. For an assumed reflector savings of 12 in., which was considered reasonable for a 10-ft diameter core, the radial peak to average factor comes out to be 1.74, neglecting reflector peaking which would tend to reduce this number. The radial peaking factor fixes the heat load for the hot channel, and this heat load together with the tube dimensions and coolant flow rate (fixed by the heat load and the desired coolant temperature rise through the core) determine the pressure drop through the hot channel. Assuming common inlet and outlet plenums and orificed tubes, this sets the reactor pressure drop. The pressure drop across the hot channel was found to be quite sensitive to heat load but, since the calculated radial peaking factor is probably conservative, this should in turn provide for conservative estimates of pressure drop and pumping power through the core.

Since pressure drop and pumping power are also sensitive to nominal coolant pressure, coolant channel tube diameter, and reactor inlet and outlet bulk temperature, these parameters were left as variables and a parametric analysis was performed with the aid of a Burroughs E101 Computer to establish the best operating conditions to minimize pumping power.

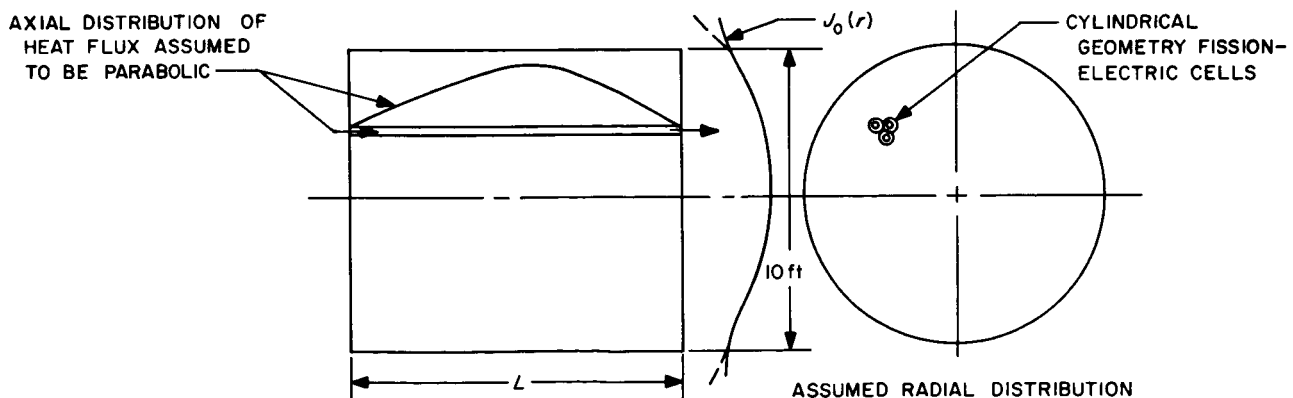


Fig. 2. Fission-electric reactor showing assumed heat-load distribution

The number of cells comprising this hypothetical reactor is also needed to fix the heat load on each cell, and is based on the following:

1. The cathode diameter is set at $1\frac{1}{2}$ times the coolant channel diameter. This is somewhat arbitrary, but provides for enough wall thickness to keep the hoop stress down to about 1000 psi for all tube diameters at an operating pressure of 500 psia, which was taken to be the maximum desirable operating pressure.
2. The vacuum gap is fixed at 1 cm. This is based on an estimate of the minimum gap necessary to avoid voltage breakdown at an assumed operating level of 10^6 v.
3. The ratio of moderator volume to total volume is fixed at 0.50.

Using these criteria, the following lattice dimensions and number of cells, Table 1, are obtained for the tube diameters considered here; see Fig. 1. The cell conversion effi-

Table 1. Various cell geometries considered in this study

D_w , in.	D_c , in.	D_a , in.	D_a/D_c	L/D_w	b , in.	n , cells
0.25	0.375	1.163	3.10	480	1.52	5,560
0.375	0.562	1.350	2.40	320	1.72	4,380
0.500	0.750	1.538	2.05	240	1.93	3,500
0.750	1.125	1.913	1.67	160	2.37	2,430
1.000	1.50	2.288	1.53	120	3.68	1,800

Table 2. Heat transfer information for cell geometries tabulated in Table 1^a

D_w , in.	Cell heat load average, $\times 10^5$ Btu/hr	Hot channel, $\times 10^5$ Btu/hr	Heat transfer area—one channel, ft^2 (total)	Average heat flux (at inner tube wall), $\times 10^5$ Btu/hr-ft ²	Flow area—one channel (total), ft^2
0.25	3.02	5.24	0.654 (3,700)	4.61	0.00034
0.375	3.89	6.76	0.983 (4,310)	9.95	0.00077 (3.37)
0.500	4.87	8.47	1.310 (4,580)	3.72	0.00136 (4.76)
0.790	7.02	12.20	1.965 (4,770)	3.57	0.00307 (7.45)
1.00	9.47	16.43	2.62 (4,720)	3.62	0.00545 (9.80)

^aThese values are based on an assumed total heat load of 500 Mw, and are therefore conservative since conversion efficiency of the cells are not taken into account. It is interesting to note that an optimum tube diameter for maximum heat transfer occurs at $D_w = 0.79$ in. The fact is verified in the Appendix that there exists an optimum geometry for maximum heat transfer area, for the criteria mentioned earlier.

ciency is a function of anode to cathode diameter ratio, D_a/D_c , and fuel layer thickness, as well as the operating voltage of the cell (Ref. 9). Curves of cell efficiency vs fuel layer thickness are reproduced in Fig. 3 for a series of diameter ratios, based on the optimum operating voltage for each case.

Pertinent heat transfer information for the different cell geometries are given in Table 2.

In the subsequent analysis it is shown that pressure drops and pumping power are also quite sensitive to the

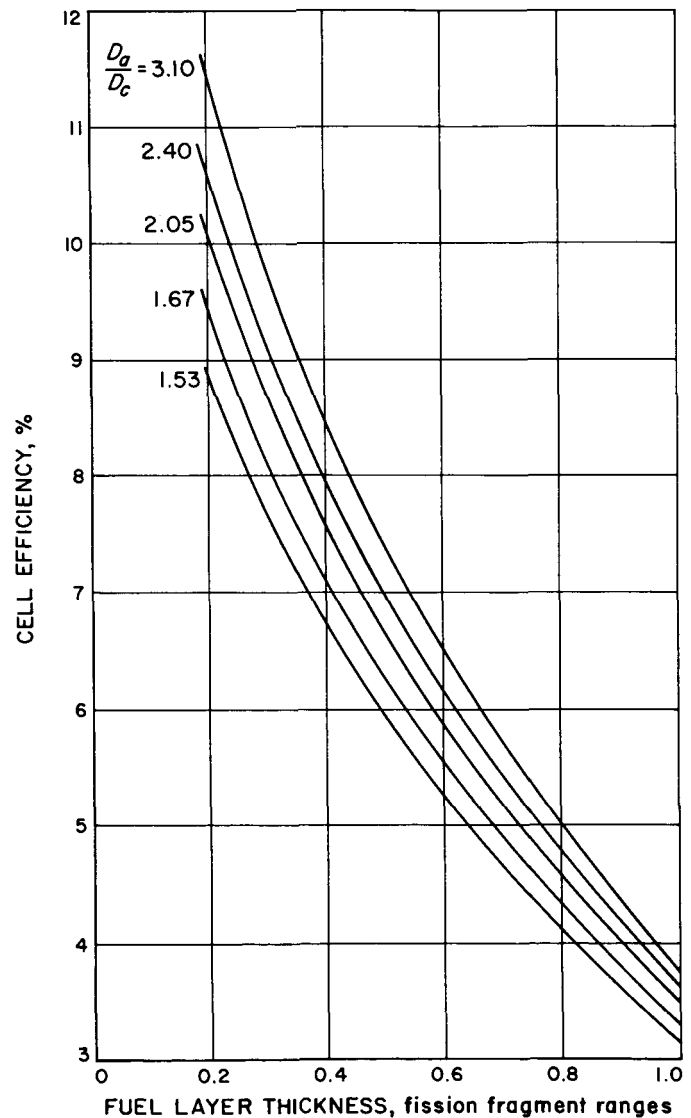


Fig. 3. Fission-electric cell conversion efficiencies vs fuel-layer thickness expressed as a fraction of mean fission fragment range for various anode-cathode diameter ratios

choice of coolant gas. Using Ref. 11 as a guide, it was decided that the most promising coolants for use in a gas-cooled fission-electric reactor were hydrogen and helium. The following data are from Ref. 11, Part 3, Table 6.1:

Relative pumping power compared to helium

H ₂	He	CO ₂	N ₂	Air	CO	A
0.17	1.0	1.8	4.0	4.0	4.0	24

CO₂, N₂, air and CO were ruled out because of high pumping power and because of their incompatibility with graphite at high temperatures. Argon is obviously not a practical choice, and its relative gamma activation is very high. Compatibility of the coolant medium with graphite at high temperature is important since graphite would seem to be the most promising high-temperature structural material (Ref. 12).

A. Reactor Temperature Distributions

1. Fluid Stagnation Temperature and Wall Temperature

Let $x/L = \epsilon$. For a parabolic distribution of heat input as shown in Fig. 4, the variation of fluid stagnation temperature $T_o(\epsilon)$, and wall temperature $T_w(\epsilon)$ can be derived in a straightforward manner, Ref. 13, p. 253. The differential equation relating heat input to stagnation temperature rise can be written as:

$$\frac{dT_o}{d\epsilon} = 4 \left(\frac{dQ}{d\epsilon} \right)_{max} (\epsilon - \epsilon^2) = c_p \frac{dT_o}{d\epsilon} \quad (1)$$

Integrating:

$$T_o - T_{o1} = \frac{4}{c_p} \left(\frac{dQ}{d\epsilon} \right)_{max} \left(\frac{1}{2} \epsilon^2 - \frac{1}{3} \epsilon^3 \right)$$

$$T_{o2} - T_{o1} = \frac{4}{c_p} \left(\frac{dQ}{d\epsilon} \right)_{max} \frac{1}{6}$$

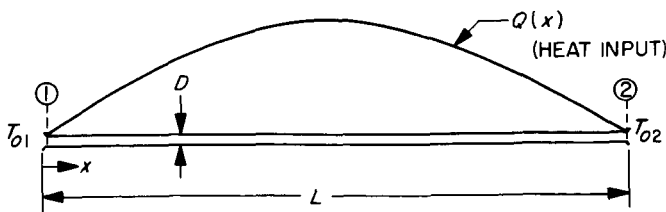


Fig. 4. Reactor tube showing parabolic distribution of heat input and nomenclature

Therefore:

$$\frac{T_o - T_{o1}}{T_{o2} - T_{o1}} = 3\epsilon^2 - 2\epsilon^3 \quad \text{Stagnation temperature variation (Fig. 5)} \quad (2)$$

and

$$\frac{dT_o}{T_{o2} - T_{o1}} = 6(\epsilon - \epsilon^2) d\epsilon \quad (3)$$

The heat balance equation for flow in the tube is:

$$\frac{\pi}{4} D^2 (\rho V) c_p dT_o = h \pi D (T_w - T_o) dx \quad (4)$$

or

$$\frac{dT_o}{T_w - T_o} = 4 \frac{h}{\rho V c_p} \frac{dx}{D} \quad (5)$$

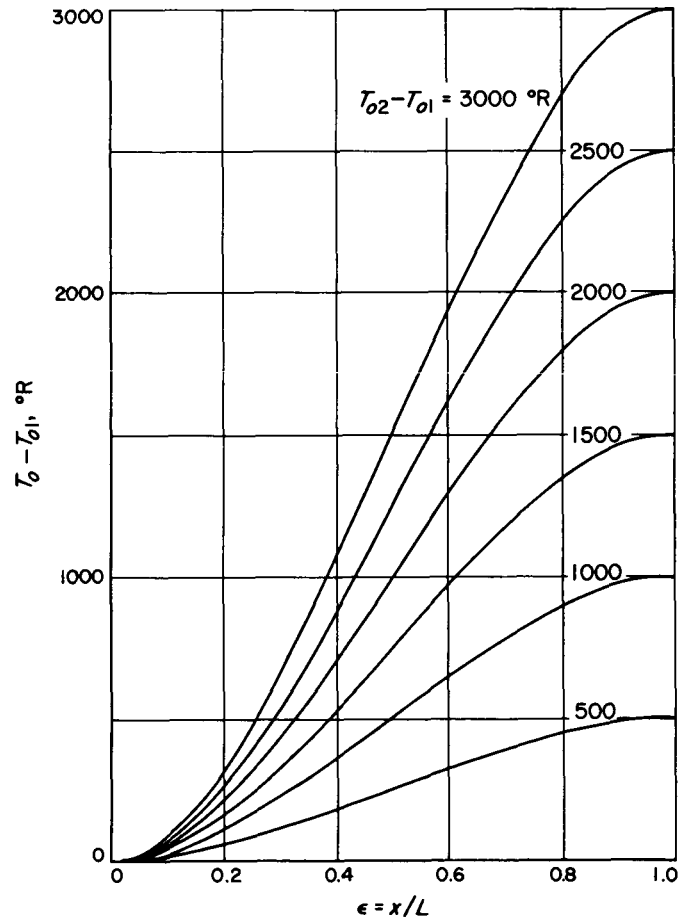


Fig. 5. Coolant stagnation temperature variation with distance into the reactor coolant channel for various values of $T_{o2} - T_{o1}$ (parabolic distribution of heat input)

Applying Reynolds Analogy⁴ between friction and heat transfer (Ref. 13, p. 243, and Ref. 3):

$$\frac{h}{(\rho V) c_p} = \frac{f}{2} \left(\frac{1}{P_r} \right)^{0.6} \quad (6)$$

Equation (5) can be written:

$$\frac{dT_o}{T_w - T_o} = 2f \frac{L}{D} \left(\frac{1}{P_r} \right)^{0.6} d\epsilon \quad (7)$$

The following identity is used:

$$\frac{T_w - T_{o1}}{T_{o2} - T_{o1}} \equiv \frac{T_w - T_o}{dT_o} \frac{dT_o}{T_{o2} - T_{o1}} + \frac{T_o - T_{o1}}{T_{o2} - T_{o1}} \quad (8)$$

which, on substitution of Eq. (2, 3 and 7) becomes:

$$\frac{T_w - T_{o1}}{T_{o2} - T_{o1}} = \frac{3(\epsilon - \epsilon^2)}{f \frac{L}{D} \left(\frac{1}{P_r} \right)^{0.6}} + \epsilon (3\epsilon - 2\epsilon^2) \quad (9)$$

Equations (2) and (9) provide⁵ the required temperature distributions, and these are plotted in Fig. 5-7 for different values of $fL/D(1/P_r)^{0.6}$.

It should be noted that the temperature distributions are relatively insensitive to the coolant gas assumed. Equation (2) shows that the coolant stagnation temperature distribution is independent of the gas used, while the wall temperature distribution is affected slightly by the Prandtl number correction in Eq. (9).

Note from Fig. 6 that values $4fL/D(1/P_r)^{0.6}$ less than 6 could lead to excessive wall temperatures for high values of T_{o2} . Table 3 gives values of this parameter for the L/D ratios considered where $P_r = (c_p \mu / k) = 0.69$ is used. This value is approximately valid for H_2 in the range 1000 to 4000°R.⁶

2. Cathode and Anode Surface Temperatures

For radial heat flow in cylinders: (See for example Ref. 14).

$$T - T_w = \frac{q_T r_o}{k} \ln \frac{r}{r_w} \quad (10)$$

where q_T is the heat flux at the cathode surface, Fig. 8.

⁴The statement of Reynolds Analogy, Eq. (6), includes the Prandtl number correction which is omitted by Shapiro, Ref. 13.

⁵Eq. (9) also corrects an error in Ref. 13, Eq. (8.69).

⁶For helium, $P_r = 0.83$ should be used for the same temperature range.

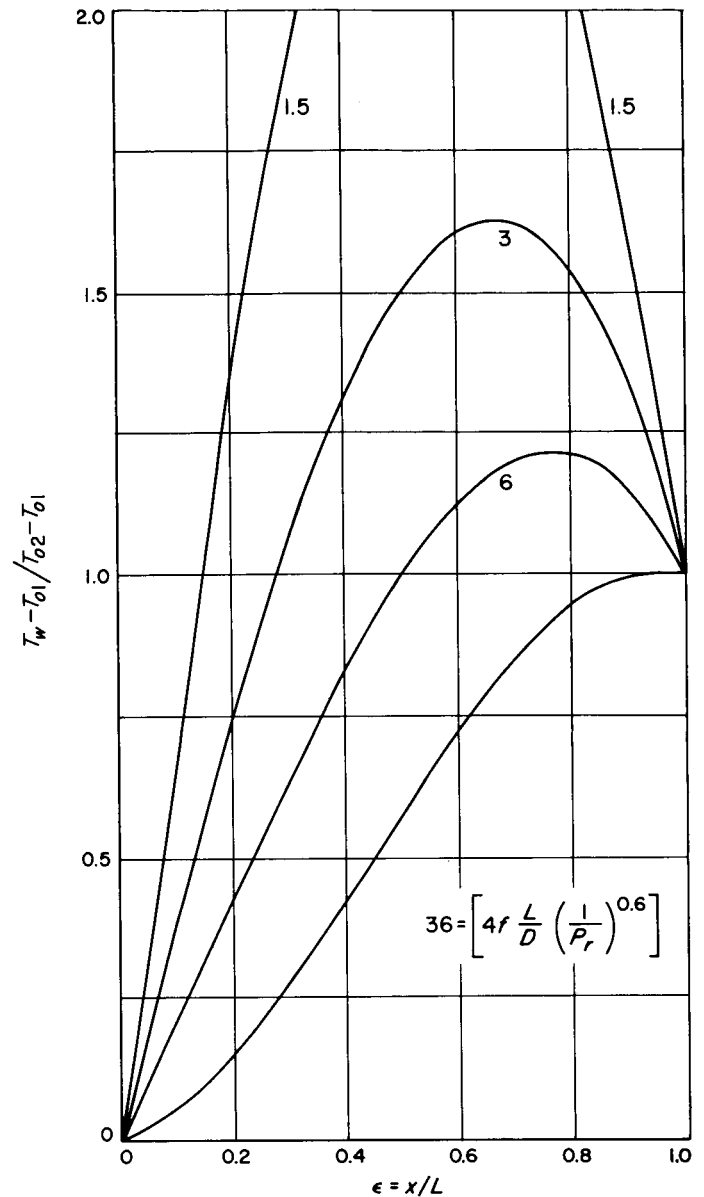


Fig. 6. Coolant channel wall temperature variation for parabolic distribution of heat input and various values of $4fL/D(1/P_r)^{0.6}$

Table 3. Values of the non-dimensional parameter $4fL/D(1/P_r)^{0.6}$ for the L/D values considered in this study

f	D_w , in. =	0.25	0.50	0.75	1.00	$(L = 10 \text{ ft})$
	$L/D_w =$	480	240	160	120	
0.005		12	6	4	3	} $4fL/D(1/P_r)^{0.6}$
0.010		24	12	8	6	
0.015		36	18	12	9	
0.020		48	24	16	12	

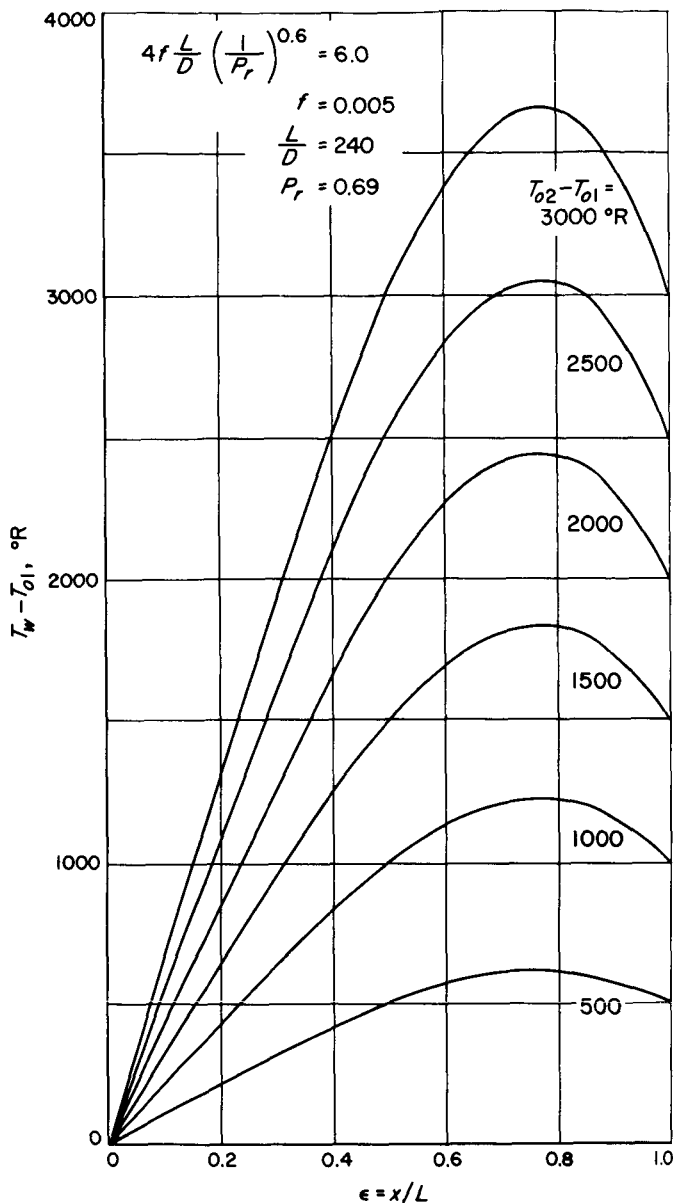


Fig. 7. Coolant channel wall temperature variation for parabolic distribution of heat input with conditions listed

It is assumed that all of the heat generation occurs in a very thin layer on the cathode and anode surfaces. This is a valid assumption since the fission fragment range is very short. In a fission cell, approximately 80% of the total heat generation occurs at the cathode surface, and 20% at the anode surface; the latter is due to fission fragment impact.

It is further assumed in this case that the heat generated at the anode is radiated back to the cathode so that

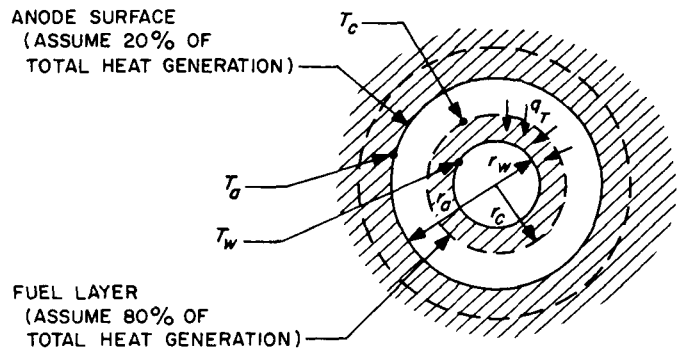


Fig. 8. Fission-electric cell cross section

all of the heat generated passes through the cathode surface (q_r Btu/ft²-hr). For $D_w = 0.50$ in., which would require 3,500 cells, the heat-load breakdown is as follows:

$$\frac{500,000}{3,500} \text{ kw} = 143 \text{ kw/cell (average)}$$

With the assumed radial peaking factor of 1.74 this means:

$$\begin{aligned} &249 \text{ kw for the hot cell} \\ &\text{or } 24.9 \text{ kw/ft (average in the hot channel)} \end{aligned}$$

Using the 1.5 axial peaking factor for parabolic axial flux distribution, this means:

$$37.4 \text{ kw/ft peak heat load in the hot channel}$$

Finally, for $D_w = 0.50$ in. ($D_c = 0.75$ in.), the cathode circumference is 0.196 ft; therefore the maximum cathode surface heat flux in the reactor is:

$$\begin{aligned} (q_r)_{max} &= \frac{37.4}{0.196} = 191 \frac{\text{kw}}{\text{ft}^2} \times 3413 \text{ Btu/hr-kw} \\ &= 6.52 \times 10^5 \text{ Btu/hr-ft}^2 \\ &\quad \text{(at cathode surface)} \end{aligned}$$

In the range 3000 to 5000°F, k for graphite is about 18 Btu/hr-ft°F.

Using Eq. (10),

$$T_c - T_w = \frac{6.52 \times 10^5}{18} \times \frac{0.750}{2 \times 12} \ln 1.5 = 459^\circ\text{F}$$

This much of a temperature difference across the tube wall would probably produce excessive thermal stresses in the tube wall. In Ref. 3, p. 27, it is shown that the maximum thermal stress in a hollow cylinder with heat

flow radially inward is a tensile stress on the inside surface of the tube. The magnitude of this stress is given by Ref. 3, Eq. (44), (see also Ref. 15):

$$(S_{th})_{tensile} = \frac{2}{3} \frac{\alpha E}{1 - \nu} (T_c - T_w) \Omega \left(\frac{t}{D} \right) \quad (11)$$

From Ref. (3) Fig. 17 for $t/D = (0.125/0.500) = 0.25$, $\Omega = 1.04$. The coefficient of thermal expansion, α , for graphite is taken as 10×10^{-6} in./in. $^{\circ}$ F, the maximum modulus of elasticity is $E_{max} = 2.3 \times 10^6$ lb/in. 2 , $\nu = 0.3$. This gives on substitution in Eq. (11):

$$S_{th} = 10,500 \text{ psi}$$

which is considerably higher than the maximum tensile hoop stress due to a 500 psia internal pressure in the tube. Obviously special consideration would have to be given to the problem of thermal stresses.

There is also the problem of thermal stresses caused by axial temperature gradients in the core. This problem has not been examined here.

To reduce thermal stresses, it might be desirable to provide for additional coolant channels between the fission-electric cells. This approach would require a two-dimensional analysis to determine the temperature distributions and thermal stresses in the solid portions of the reactor. The problem has been set aside for the present.

The equation for radiation heat transfer between two concentric cylinders (outer cylinder to inner cylinder) Ref. 16, p. 206; Ref. 17, p. 242, as applied to this problem is:

$$Q_r = 0.173 A_c F_{12} \left[\left(\frac{T_a}{100} \right)^4 - \left(\frac{T_c}{100} \right)^4 \right] \quad (12)$$

where the shape factor F_{12} is represented by:

$$\frac{1}{F_{12}} = \frac{1}{F_{ca}} + \frac{1}{\epsilon_c} - 1 + \frac{A_c}{A_a} \left(\frac{1}{\epsilon_a} - 1 \right)$$

The ϵ 's in the above expression are surface emissivities, and the F_{ca} is a black body shape factor. Assuming the emissivity of the cathode and anode surfaces to be 0.9 ($\epsilon_a = \epsilon_c = 0.9$) and taking the black body shape factor

F_{ca} to be 1.0, since in this case all heat lost by the anode goes to the cathode:

$$\frac{1}{F_{12}} = \frac{1}{1} + \frac{1}{0.9} - 1 + \frac{0.75}{1.538} \left(\frac{1}{0.7} - 1 \right) = 1.16$$

Assume that the friction factor $f = 0.005$, then for $D_w = 0.500$ in., $L/D_w = 240$, $P_r = 0.69$, $4fL/D(1/P_r)^{0.6} = 6$ and from Fig. 6, for $T_{o2} - T_{o1} = 2000^{\circ}$ F, obtain

$$(T_w - T_{o1})_{max} = 1.225 \times 2000 = 2450^{\circ}\text{R}$$

or

$$(T_w)_{max} = 4450^{\circ}\text{R, for } T_{o1} = 2000^{\circ}\text{R}$$

Using the 459° F temperature drop across the tube wall, obtained earlier:

$$(T_c)_{max} = 4450 + 459 = 4909^{\circ}\text{R}$$

If 20% of the total heat is generated at the anode surface, by using the 37.4 kw/ft peak hot channel heat load obtained earlier, the Q_r input to Eq. (12) is:

$$Q_r = 0.20 \times (37.4 \times 3,413) = 2.55 \times 10^4 \text{ Btu/hr-ft}$$

and $A_c = (\pi \times 0.75/12) \times 1.0 = 0.1962 \text{ ft}^2/\text{ft}$ of tube length. So that, using Eq. (12)

$$2.55 \times 10^4 = 0.173 \times 0.1962 \times \frac{1}{1.16} \left[\frac{T_a^4}{100} - (4909)^4 \right]$$

$$(T_a)_{max} = 5090^{\circ}\text{R} = 4630^{\circ}\text{F}$$

and this should be the peak temperature in the core. As shown above, cooling of the anodes by radiation heat transfer to the cathodes should impose only a minor temperature difference (180° F) between anode and cathode at the suggested operating temperature. However, because of the thermal stress problem pointed out earlier, it would be desirable to remove some of the peak heat load from the cathode coolant channels either by power flattening or by providing additional coolant channels between or in the anodes. This would have the effect of lowering the temperature difference across the cathode tube wall and thereby would reduce the thermal tensile stress on the inner tube wall. Additional coolant channels would also tend to reduce the pumping power through the core.

The attraction to having no coolant channels between the anodes is of course the fact that the number of coolant channels is greatly reduced. This could be important when one considers the mechanical complexity involved in the variety of access channels that must be designed into at least one end of a fission cell reactor. For example, the vacuum channels would probably have to be vented to outer space to remove accumulations of fission produce gases. Also, space would probably have to be allowed for control rods and for the coolant channels servicing the driver fuel modules. The variety of access channels that would have to be provided would seem to require that the coolant channels be fed by individual pressure tubes, thus making it extremely desirable to keep the total number of tubes down to a minimum.

Another advantage to having no coolant channels between the anodes is that the radial temperature gradients in the anode structure could be made negligibly small. By suitable orificing of the coolant channels, each tube could be made to have the same axial temperature distribution. And, since fission heat generation in the anode occurs only at the anode surface and is removed only at the anode surface, the anode structure at any specified axial position should operate at the same uniformly high temperature and would not be required to sustain significant temperature gradients.

Temperature gradients due to gamma and fast neutron heating are not expected to be significant. If it is assumed that 10% of the total reactor thermal rating is due to gamma and fast neutron heating and is uniformly distributed throughout the solid portion of the core, this amounts to only 70 w/in³ and results in temperature gradients on the order of 3°F in 0.1 in. in graphite.

B. Reactor Pressure Drop and Pumping Power

1. Pressure Drop

The applicable differential equation for compressible flow at constant mass flow rate and constant specific heat and molecular weight, in a constant area duct, with friction and heat transfer, is (Ref. 13, Chap. 8):

$$\frac{dp_o}{p_o} = -\frac{\gamma M^2}{2} \left(\frac{dT_o}{T_o} + 4f \frac{dx}{D} \right) \quad (13)$$

Applying Reynold's Analogy between friction and heat transfer, known integral relations between gas properties at two cross sections, and a simplifying approximation

valid for low Mach number flow, Eq. (13) can be readily integrated to obtain the following useful relationships:⁷

$$1 - \left(\frac{p_{o2}}{p_{o1}} \right)^2 = \gamma M_1^2 B_1 \mathcal{Q}_1 \left(4f \frac{L}{D} \right) \quad (14)$$

where

$$B_1 = \frac{1}{2} \left[1 + \left(\frac{p_{o2}}{p_{o1}} \right)^2 \frac{T_{o1}}{T_{o2}} \frac{M_2^2}{M_1^2} \right] \quad (15)$$

and

$$\mathcal{Q}_1 = \int_0^1 \frac{T_o}{T_{o1}} \left[\frac{1}{2} \frac{T_w - T_o}{T_o} \left(\frac{1}{P_r} \right)^{0.6} + 1 \right] d \left(\frac{x}{L} \right) \quad (16)$$

or

$$\left(\frac{p_{o1}}{p_{o2}} \right)^2 - 1 = \gamma M_2^2 B_2 \mathcal{Q}_2 \left(4f \frac{L}{D} \right) \quad (17)$$

where

$$B_2 = \frac{1}{2} \left[1 + \left(\frac{p_{o1}}{p_{o2}} \right)^2 \frac{T_{o2}}{T_{o1}} \frac{M_1^2}{M_2^2} \right] \quad (18)$$

and

$$\mathcal{Q}_2 = \int_0^1 \frac{T_o}{T_{o2}} \left[\frac{1}{2} \frac{T_w - T_o}{T_o} \left(\frac{1}{P_r} \right)^{0.6} + 1 \right] d \left(\frac{x}{L} \right) \quad (19)$$

Either Eq. (14) or (17), above, can be used depending on whether conditions at the tube inlet or outlet, respectively, are used. The low Mach number simplification applied above is valid for this case since tube outlet Mach numbers of about 0.2 or higher were found to give unacceptably high pressure drops. On p. 250 of Ref. 13 it is shown that if Mach number never exceeds 0.3, the error in Δp_o is at most a few percent.

For calculating reactor pressure drops, conditions at the reactor outlet were specified (i.e., p_{o2} and T_{o2}) so that Eq. (17) is used. It is seen that \mathcal{Q}_2 is a function of the temperature distributions T_o and T_w which are given by Eq. (2) and (9). Eq. (9) is a function of the tube position parameter ϵ and the parameter $f(L/D)(1/P_r)^{0.6}$ as well as the specified entrance and exit bulk temperatures T_{o1} and T_{o2} .

In Table A-1 in the Appendix, \mathcal{Q}_1 and \mathcal{Q}_2 are evaluated for both hydrogen and helium for the values of L/D to be used in the subsequent analysis, with the result shown in Table 4.

⁷See Appendix and Ref. 13, p. 249, for details.

Table 4. Tabulation of parameters \mathcal{Q}_1 and \mathcal{Q}_2 in terms of bulk inlet and outlet temperatures, for use in Eq. (14 and 17)

D , in.	L/D	$4f L/D \left(\frac{1}{Pr}\right)^{0.6}$	$(\mathcal{Q}_2 - 1) \frac{T_{o2}}{T_{o2} - T_{o1}}$	$4f L/D \left(\frac{1}{Pr}\right)^{0.6}$	$(\mathcal{Q}_2 - 1) \frac{T_{o2}}{T_{o2} - T_{o1}}$
			or $(\mathcal{Q}_1 - 1) \frac{T_{o1}}{T_{o2} - T_{o1}}$		or $(\mathcal{Q}_1 - 1) \frac{T_{o1}}{T_{o2} - T_{o1}}$
0.25	480	12.0	0.604	10.75	0.619
0.375	320	8.0	0.657	7.16	0.679
0.500	240	6.0	0.709	5.37	0.738
0.790	152	3.8	0.834	3.41	0.847
1.00	120	3.0	0.916	2.69	1.003
Hydrogen				Helium	

In Table 4, Prandtl numbers ($c_p \mu / k$) of 0.69 for hydrogen and 0.83 for helium were used. These values represent the mean value of Prandtl number in the temperature range 1000 to 4000°R and are very nearly constant in this temperature range.

Also, Table 4 is based on a friction factor, f , of 0.005 for both hydrogen and helium. This number is approximately valid for turbulent subsonic compressible flow in smooth tubes for Reynolds numbers⁸ between 10^4 and 10^5 .

The ratio of specific heats, $\gamma (= c_p / c_v)$ used in Eq. (14) and (17) is taken to be constant. For hydrogen $\gamma = 1.4$ is approximately valid for the temperature range 1000 to 4000°R (Ref. 12, and Ref. 3, Fig. 1). For helium the specific heat ratio is very nearly the same as for hydrogen (Ref. 12) so that $\gamma = 1.4$ is used for both gases.

The exit Mach number expression for use in Eq. (17) is obtained as follows:

$$M_2 = \frac{V_2}{c_2} = \frac{V_2}{\left(\frac{\gamma p_2 g_c}{\rho_2}\right)^{1/2}} = \frac{V_2}{(\gamma R T_2 g_c)^{1/2}}$$

$$= \frac{G}{\rho_2 (\gamma R T_2 g_c)^{1/2}} = \frac{G}{p_2} \left(\frac{R T_2}{\gamma g_c}\right)^{1/2} \quad (20)$$

*See, for example, Ref. 13, Chapter 28, and Ref. 5, Fig. 8 which gives experimental verification for hydrogen and helium of the Karman-Nikuradse formula for friction factor in the Reynolds' number range 10^3 to 10^5 . Ref. 5, however, indicates that a friction factor of 0.006 would be more accurate for Reynolds numbers between 10^4 to 10^5 .

where, as an approximation the perfect gas equation of state is assumed to be valid.⁹

In Eq. (20), the channel exit temperature T_2 and pressure p_2 are taken to be equal to the assumed stagnation temperature T_{o2} and stagnation pressure p_{o2} . This is a valid approximation for low Mach numbers since: (Ref. 13, p. 83)

$$T_{o2} = T_2 \left(1 + \frac{\gamma - 1}{2} M_2^2\right) \approx T_2 \text{ for } M_2 \text{ small} \quad (21)$$

$$p_{o2} = p_2 \left(1 + \frac{\gamma - 1}{2} M_2^2\right)^{\gamma/\gamma - 1} \approx p_2 \text{ for } M_2 \text{ small} \quad (22)$$

The mass flow rate per unit area, G (lbm/ft² sec) is determined by the known heat load in the channel (Q_c Btu/hr), the channel area (A_c), the specified temperature differential ($T_{o2} - T_{o1}$), and the coolant specific heat (c_p Btu/lbm-°R). The heat loads are tabulated in Table 2.

$$G = \frac{Q_c}{c_p A_c (T_{o2} - T_{o1}) \times 3600} \quad (23)$$

where

$$c_p \text{ for } H_2 = 3.6 \text{ Btu/lbm-°R (Ref. 3, Fig. 1)}$$

$$c_p \text{ for He} = 1.7 \text{ Btu/lbm-°R (Ref. 12, page 33)}$$

*This is a typical assumption. See, for example, Ref. 3. Furthermore, Eq. (13) is based on the assumption of a perfect gas.

The following gas constants are used in Eq. (20):

$$R \text{ for } H_2 = 772 \text{ ft-lbf/lbm-}^\circ R$$

$$R \text{ for He} = 386 \text{ ft-lbf/lbm-}^\circ R$$

The correct value of (p_{o1}/p_{o2}) is obtained through an iterative process. In Eq. (17) B_2 is taken to be equal to 1.0 to obtain an estimate of (p_{o1}/p_{o2}) . A value of B_2 is then obtained using Eq. (18). A corrected value of (p_{o1}/p_{o2}) is then found and the process is repeated until convergence is obtained. In most cases the second approximation has been found to be adequate since B_2 is very nearly equal to 1.0 for low Mach numbers.

Using the above information, reactor hot channel pressure drops were calculated with the aid of a Burroughs E101 Computer for the following combinations of variables:

1. $D_w = 0.500$ in., $p_{o2} = 100, 200, 250, 300, 400$ and 500 psia

for $T_{o2} = 4000^\circ R$, $\Delta T_o = 3000, 2500$ and $2000^\circ R$

$T_{o2} = 3500^\circ R$, $\Delta T_o = 2500, 2000$ and $1500^\circ R$

$T_{o2} = 3000^\circ R$, $\Delta T_o = 2000, 1500$ and $1000^\circ R$

2. $p_{o2} = 250$ psia, $D_w = 0.25, 0.375, 0.500, 0.790$ and 1.00 in. for the same temperature combinations as in Set 1.

The above runs were performed for H_2 and for He coolant gases. The results of the pressure drop calculations are tabulated in Tables 5-8.

It was found that the reactor hot-channel pressure drops tabulated in Tables 5-8 could be considerably greater than the average channel pressure drops. For instance, a calculation was carried out of the average channel pressure drop for the case $D_w = 500$ in., $T_{o2} = 4000^\circ R$, $\Delta T_o = 2500^\circ R$, and a value of about 8 psia obtained. This should be compared with the value of 22.68 psia for the hot channel for the same inlet and outlet temperatures, and tube diameter (Table 5). The pumping power based on the hot channel pressure drop comes out to be 7.31 Mw, whereas if the reactor radial power distribution were absolutely flat the pumping power could be reduced by about a factor of 3, thus showing the value of power flattening in reducing pumping power.

Table 5. Results of reactor pressure drop calculations, hydrogen, $D_w = \text{constant} = 0.50$ in.

$T_{o2} =$		$(j = 1)^a$ 4000°R			$(j = 2)$ 3500°R			$(j = 3)$ 3000°R		
$(T_{o2} - T_{o1}) =$		$(k = 1)^a$ 3000	$(k = 2)$ 2500	$(k = 3)$ 2000	$(k = 2)$ 2500	$(k = 3)$ 2000	$(k = 4)$ 1500	$(k = 3)$ 2000	$(k = 4)$ 1500	$(k = 5)$ 1000
$p_{o2} = 100$ psia ($l = 1$) ^a	M_2	0.29146	0.34975	0.43719	0.32716	0.40895	0.54527	0.37861	0.50482	0.75723
	M_1	0.103	0.138	0.176	0.117	0.160	0.200	0.134	0.180	0.210
	p_{o1}/p_{o2}	1.3560	1.4544	1.6140	1.4267	1.5783	1.8225	1.5269	1.7501	2.1590
	Δp_o	35.60 psia	45.43	61.40	42.67	57.83	82.25	52.69	75.01	115.90
$p_{o2} = 200$ ($l = 2$)	M_2	0.14573	0.17487	0.21859	0.16358	0.20447	0.27263	0.18931	0.25241	0.37861
	M_1	0.0655	0.0835	0.1275	0.077	0.112	0.157	0.093	0.138	0.202
	p_{o1}/p_{o2}	1.1031	1.1378	1.1954	1.1264	1.1787	1.2784	1.1622	1.2491	1.4625
	Δp_o	20.61	27.56	39.08	25.27	35.75	55.68	32.44	49.82	92.50
$p_{o2} = 250$ ($l = 3$)	M_2	0.11658	0.13990	0.17487	0.13086	0.16358	0.21811	0.15145	0.20193	0.30289
	M_1	0.055	0.0785	0.109	0.064	0.0955	0.137	0.0781	0.120	0.180
	p_{o1}/p_{o2}	1.0682	1.0907	1.1302	1.0825	1.1190	1.1881	1.1065	1.1681	1.3156
	Δp_o	17.04	22.68	32.54	20.61	29.75	47.02	26.63	42.02	78.89
$p_{o2} = 300$ ($l = 4$)	M_2	0.09715	0.11658	0.14573	0.10905	0.13632	0.18176	0.12620	0.16827	0.25241
	M_1	0.046	0.0665	0.094	0.055	0.082	0.118	0.067	0.106	0.1625
	p_{o1}/p_{o2}	1.0471	1.0633	1.0920	1.0584	1.0839	1.1320	1.0751	1.1214	1.2303
	Δp_o	14.12	18.98	27.61	17.52	25.16	39.61	22.53	36.41	69.10
$p_{o2} = 400$ ($l = 5$)	M_2	0.07286	0.08744	0.10930	0.08179	0.10244	0.13632	0.09465	0.12620	0.18931
	M_1	0.035	0.051	0.073	0.0425	0.063	0.096	0.052	0.083	0.135
	p_{o1}/p_{o2}	1.0266	1.0359	1.0527	1.0335	1.0475	1.0787	1.0431	1.0697	1.1384
	Δp_o	10.64	14.37	21.07	13.38	19.01	31.49	17.23	27.88	55.38
$p_{o2} = 500$ ($l = 6$)	M_2	0.05829	0.06995	0.08744	0.06543	0.08179	0.10905	0.07572	0.10096	0.15145
	M_1	0.028	0.041	0.059	0.034	0.052	0.0786	0.042	0.068	0.112
	p_{o1}/p_{o2}	1.0169	1.0230	1.0338	1.0213	1.0311	1.0509	1.0276	1.0452	1.0900
	Δp_o	8.473	11.49	16.88	10.64	15.57	25.25	13.82	22.58	45.01

^ai, j, k, l refer to computer program indices.

Table 6. Results of reactor pressure drop calculations, helium, $D_w = \text{constant} = 0.50 \text{ in.}$

$T_{o2} =$		$(j = 1)$ 4000°R			$(j = 2)$ 3500°R			$(j = 3)$ 1500°R		
$(T_{o2} - T_{o1}) =$		$(k = 1)$ 3000°R	$(k = 2)$ 2500	$(k = 3)$ 2000	$(k = 2)$ 2500	$(k = 3)$ 2000	$(k = 4)$ 1500	$(k = 3)$ 2000	$(k = 4)$ 1500	$(k = 5)$ 1000
$p_{o2} = 100 \text{ psia}$ $(l = 1)$	M_2	0.43745	0.52494	0.65617	0.49103	0.61379	0.81839	0.56826	0.75768	
	M_1	0.120	0.153	0.182	0.130	0.169	0.184	0.145	0.173	0.171
	p_{o1}/p_{o2}	1.6901	1.8426	2.0697	1.7922	2.0263	2.3169	1.9573	2.2415	2.8017
	Δp_o	69.01 psia	84.26	106.97	79.22	102.63	131.69	95.73	124.15	180.17
$p_{o2} = 200$ $(l = 2)$	M_2	0.21872	0.26247	0.32809	0.24552	0.30690	0.40920	0.28413	0.37884	0.56826
	M_1	0.088	0.121	0.159	0.0974	0.143	0.188	0.117	0.169	0.223
	p_{o1}/p_{o2}	1.2210	1.2869	1.3691	1.2565	1.3701	1.5479	1.3295	1.5007	1.8490
	Δp_o	44.20	57.34	79.22	51.30	74.03	109.59	65.91	100.14	169.79
$p_{o2} = 250$ $(l = 3)$	M_2	0.17498	0.20998	0.26247	0.19641	0.24552	0.32736	0.22730	0.30307	0.45461
	M_1	0.076	0.106	0.140	0.087	0.125	0.170	0.105	0.152	0.210
	p_{o1}/p_{o2}	1.1484	1.1943	1.2676	1.1775	1.2488	1.3781	1.2285	1.3441	1.6061
	Δp_o	37.10	48.57	66.89	44.37	62.20	94.53	57.13	86.03	151.53
$p_{o2} = 300$ $(l = 4)$	M_2	0.14582	0.17498	0.21872	0.16368	0.20460	0.27280	0.18942	0.25256	0.37884
	M_1	0.065	0.093	0.125	0.077	0.112	0.156	0.093	0.137	0.200
	p_{o1}/p_{o2}	1.1038	1.1390	1.1937	1.1283	1.1811	1.2797	1.1646	1.2503	1.4623
	Δp_o	31.15	41.69	58.10	38.48	54.33	83.90	49.38	75.09	138.68
$p_{o2} = 400$ $(l = 5)$	M_2	0.10936	0.13123	0.16404	0.12276	0.15345	0.20460	0.14207	0.18942	0.28413
	M_1	0.051	0.074	0.104	0.0605	0.0905	0.130	0.074	0.115	0.175
	p_{o1}/p_{o2}	1.0599	1.0809	1.1171	1.0738	1.1065	1.1677	1.0954	1.1517	1.2871
	Δp_o	23.97	32.36	46.85	29.53	42.58	67.08	38.18	60.68	114.85
$p_{o2} = 500$ $(l = 6)$	M_2	0.08749	0.10499	0.13123	0.09821	0.12276	0.16368	0.11365	0.15154	0.22730
	M_1	0.0415	0.0605	0.085	0.0495	0.075	0.112	0.0615	0.097	0.153
	p_{o1}/p_{o2}	1.0386	1.0522	1.0752	1.0478	1.0694	1.1130	1.0625	1.1002	1.1941
	Δp_o	19.31	26.11	37.60	23.88	34.72	56.50	31.27	50.09	97.07

Table 7. Results of reactor pressure drop calculations, hydrogen, $p_{o2} = \text{constant} = 250 \text{ psia}$

$T_{o2} =$		4000°R $j = 1$			3500°R $j = 2$			3000°R $j = 3$		
$T_{o2} - T_{o1} =$		3000°R	2500	2000	2500	2000	1500	2000	1500	1000
$D_w = 0.25 \text{ in.}$ $(i = 1)$	M_2	0.2888	0.3465	0.4332	0.3242	0.4053	0.5403	0.3752	0.5003	0.7504
	M_1	0.086	0.114	0.140	0.097	0.126	0.155	0.108	0.142	0.1575
	p_{o1}/p_{o2}	1.5975	1.7639	2.0050	1.7158	1.9331	2.3202	1.8638	2.2123	2.8194
	Δp_o	149.37 psia	190.98	251.24	178.95	233.28	330.05	215.95	303.08	454.86
$D_w = 0.375 \text{ in.}$ $(i = 2)$	M_2	0.1638	0.1966	0.2457	0.1837	0.2298	0.3065	0.2128	0.2837	0.4256
	M_1	0.069	0.098	0.130	0.081	0.114	0.158	0.095	0.138	0.190
	p_{o1}/p_{o2}	1.1626	1.2184	1.3044	1.2001	1.2768	1.4331	1.2509	1.3835	1.6806
	Δp_o	40.64	54.60	76.11	50.03	69.20	108.26	62.72	95.86	170.14
$D_w = 0.500 \text{ in.}$ $(i = 3)$	M_2	0.1166	0.1399	0.1749	0.1309	0.1636	0.2181	0.1514	0.2019	0.3029
	M_1	0.055	0.0785	0.109	0.064	0.0953	0.137	0.0781	0.120	0.180
	p_{o1}/p_{o2}	1.0682	1.0907	1.1302	1.0825	1.1190	1.1881	1.1065	1.1681	1.3156
	Δp_o	17.04	22.68	32.54	20.61	29.75	47.02	26.63	42.02	78.89
$D_w = 0.79 \text{ in.}$ $(i = 4)$	M_2	0.07442	0.08930	0.1116	0.08353	0.1044	0.1392	0.09667	0.1289	0.1933
	M_1	0.036	0.053	0.076	0.042	0.065	0.100	0.054	0.087	0.142
	p_{o1}/p_{o2}	1.0175	1.0253	1.0368	1.0226	1.0331	1.0546	1.0304	1.0490	1.0957
	Δp_o	4.39	6.33	9.21	5.64	8.28	13.65	7.60	12.24	23.93
$D_w = 1.00 \text{ in.}$ $(i = 5)$	M_2	0.05629	0.06755	0.08443	0.06318	0.07898	0.1053	0.07312	0.09749	0.1462
	M_1	0.028	0.041	0.058	0.033	0.050	0.077	0.042	0.067	0.114
	p_{o1}/p_{o2}	1.0090	1.0120	1.0171	1.0109	1.0156	1.0254	1.0145	1.0229	1.0458
	Δp_o	2.24	3.00	4.28	2.73	3.89	6.35	3.62	5.72	11.44

Table 8. Results of reactor pressure drop calculations, helium, $p_{o2} = \text{constant} = 250 \text{ psia}$

$T_{o2} =$		4000°R			3500°R			3000°R		
$T_{o2} - T_{o1} =$		3000°R	2500	2000	2500	2000	1500	2000	1500	1000
$D_w = 0.25 \text{ in.}$ ($i = 1$)	M_2	0.4322	0.5186	0.6483	0.4851	0.6064	0.8085	0.5614	0.7486	1.1228
	M_1	0.094	0.120	0.140	0.103	0.130	0.139	0.113	0.132	0.127
	p_{o1}/p_{o2}	2.0862	2.3366	2.6769	2.2629	2.6030	3.0332	2.5046	2.9239	3.7361
	Δp_o	271.55 psia	334.14	419.23	315.72	400.74	508.31	376.14	480.97	684.04
$D_w = 0.375 \text{ in.}$ ($i = 2$)	M_2	0.2456	0.2947	0.3684	0.2757	0.3446	0.4595	0.3190	0.4254	0.6381
	M_1	0.089	0.122	0.155	0.101	0.138	0.175	0.116	0.160	0.200
	p_{o1}/p_{o2}	1.3385	1.4425	1.5966	1.4052	1.5497	1.7943	1.5018	1.7350	2.1970
	Δp_o	84.62	110.62	149.15	101.30	137.42	198.59	125.45	183.74	299.26
$D_w = 0.500 \text{ in.}$ ($i = 3$)	M_2	0.1750	0.2100	0.2625	0.1964	0.2455	0.3274	0.2273	0.3031	0.4546
	M_1	0.076	0.106	0.140	0.087	0.125	0.170	0.105	0.152	0.200
	p_{o1}/p_{o2}	1.1484	1.1943	1.2676	1.1775	1.2488	1.3781	1.2285	1.3441	1.6061
	Δp_o	37.10	48.57	66.89	44.37	62.20	94.53	57.13	86.03	151.53
$D_w = 0.79 \text{ in.}$ ($i = 4$)	M_2	0.1115	0.1338	0.1673	0.1252	0.1565	0.2086	0.1449	0.1932	0.2897
	M_1	0.053	0.077	0.108	0.063	0.094	0.139	0.078	0.123	0.191
	p_{o1}/p_{o2}	1.0425	1.0569	1.0812	1.0523	1.0743	1.1185	1.0681	1.1080	1.2035
	Δp_o	10.63	14.23	20.30	13.08	18.57	29.63	17.02	27.00	50.88
$D_w = 1.00 \text{ in.}$ ($i = 5$)	M_2	0.08433	0.1012	0.1265	0.09466	0.1183	0.1578	0.1095	0.1461	0.2191
	M_1	0.041	0.060	0.085	0.049	0.0745	0.113	0.0605	0.098	0.162
	p_{o1}/p_{o2}	1.0205	1.0275	1.0391	1.0253	1.0362	1.0583	1.0327	1.0524	1.1022
	Δp_o	5.13	6.87	9.77	6.33	9.05	14.56	8.17	13.09	25.54

2. Pumping Power

There are several ways of estimating the pumping power through the reactor. Some of the possible approaches are outlined below:

$$1. Q_f \approx W \frac{\Delta p_f}{\rho_{avg}} \quad (24)$$

2. The frictional work can be obtained by integrating the tube wall shear stress \times the coolant velocity over the length of the channel:

$$dQ_f = T_w (\pi D_w dx) V$$

$$T_w = \frac{f_p V^2}{2g_c}$$

$$dQ_f = \frac{f}{2g_c} (\pi D dx) \rho V^3$$

Integrating:

$$Q_f = \frac{\pi D_a L}{2g_c} f \rho_1 V_1^3 \int_0^1 \frac{\rho}{\rho_1} \left(\frac{V}{V_1} \right)^3 d \left(\frac{V}{V_1} \right) \quad (25)$$

3. The pumping power can be computed from the work that would be required to compress the total mass flow of gas through the reactor pressure differential Δp_o to reactor inlet conditions of temperature and

pressure. For a perfect gas, the change in specific enthalpy is given by:

$$\Delta h = c_p (t_2 - t_1) = c_p t_2 \left(1 - \frac{t_1}{t_2} \right) \quad (26)$$

and for an isentropic compression process:

$$\frac{t_2}{t_1} = \left(\frac{p_2}{p_1} \right)^{\gamma-1/\gamma} \quad (27)$$

so that:¹⁰

$$\Delta h = c_p t_2 \left[1 - \left(\frac{p_1}{p_2} \right)^{\gamma-1/\gamma} \right] \left(\frac{\text{Btu}}{\text{lbm}} \right) \quad (28)$$

If W = total mass flow rate in lbm/hr, and $t_2 = T_{o1}$, $p_1 = p_{o2}$, $p_2 = p_{o1}$, then the ideal pumping power¹¹ required to overcome friction is given by:

$$Q_f (\text{Mw}) = W c_p T_{o1} \left[1 - \frac{1}{\left(\frac{p_{o1}}{p_{o2}} \right)^{\gamma-1/\gamma}} \right] \times \frac{1}{3.413 \times 10^6 \text{ Btu/hr} - \text{Mw}} \quad (29)$$

¹⁰See Ref. 18, page 42.

¹¹To estimate the actual power required to drive the compressor the above estimate would then have to be divided by the product of the compressor efficiency, usually about 0.90, and the driver efficiency, ≈ 0.80 for turbines and ≈ 0.95 for electric motors.

where

$$W = \frac{\text{Reactor thermal power in Btu/hr}}{c_p (T_{o2} - T_{o1})} \quad (30)$$

All three of the above Approaches (1, 2, and 3), have been tried for a few specific cases and it was found that the resultant pumping power estimates agreed quite well. Approach 2 has a distinct disadvantage in that the distribution of properties along the channel must first be determined. Approach 1 is only a rough approximation. It was decided that Approach 3 above was the most convenient to use since the pressure ratio (p_{o1}/p_{o2}) obtained earlier could be applied directly to obtain the desired result. Eq. (29) was programmed into the Burroughs E101 Computer and the results are plotted in Fig. 9-14 for $D_w = 0.500$ in. with p_{o2} , T_{o2} , and T_{o1} as parameters and in Fig. 15-20 for $p_{o2} = 250$ psi with D_w , T_{o2} , and T_{o1} as parameters.¹² As a further check on the accuracy of the

¹²The computer results agree with a checkpoint as shown in Fig. 9.

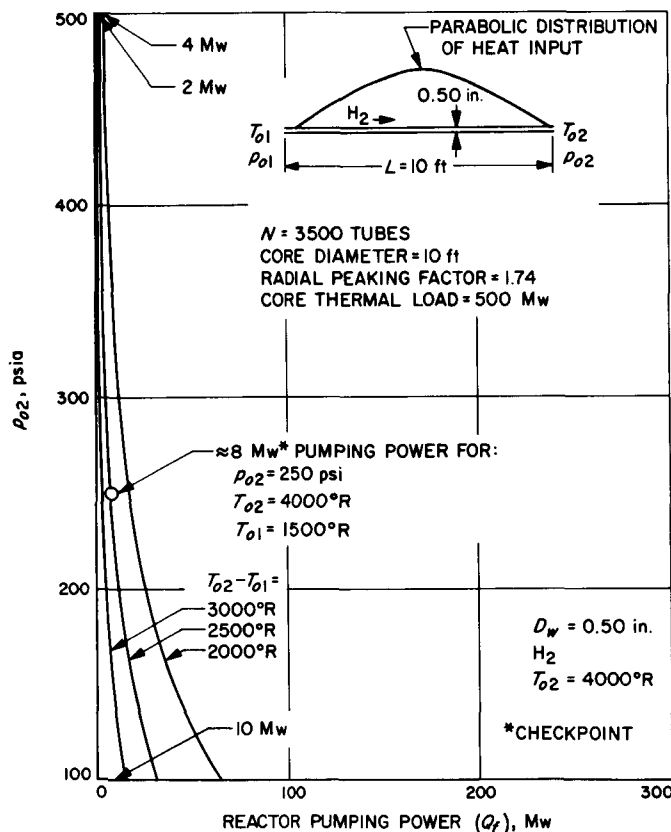


Fig. 9. Reactor pumping power parametric study at 4000°R, with H₂

pumping power results shown in Fig. 9-20, an order of magnitude estimate of the pumping power for gas cooled reactors can be obtained from the *Reactor Handbook* (Ref. 19) in which the following equation for estimating pumping power W in terms of coolant properties and reactor size is given:

$$\frac{W}{Q} = \frac{1}{Jg} \left[\frac{Q^2 L^2}{V_m^2 \Delta T^2 \Delta t} \right] \left[\frac{\eta}{c_p^2 d^2 k P_r^{0.4}} \right] \quad (31)$$

where

$$Q = \text{reactor heat load} = 1.708 \times 10^9 \text{ Btu/hr}$$

$$L = \text{core length} = 10 \text{ ft}$$

$$V_m = \text{core volume occupied by coolant} = 4.44 \text{ ft}^3 \times 10 \text{ ft} = 44.4 \text{ ft}^3$$

$$\Delta T = T_{o2} - T_{o1} = 2500^\circ\text{F}$$

$$\Delta t = (T_w - T_o) \text{ avg} \approx 752^\circ\text{F}$$

$$\eta = \text{coolant viscosity (avg)} \approx 0.50 \text{ lbm/hr-ft}$$

$$c_p = \text{specific heat} = 3.6 \text{ Btu/lbm-}^\circ\text{R}$$

$$k = \text{thermal conductivity} = 0.275 \frac{\text{Btu}}{\text{hr-ft}} \cdot ^\circ\text{R}$$

$$d = \text{gas density} = 0.0192 \text{ lbm/ft}^3 \text{ (@ 250 psia)}$$

$$P_r = \text{Prandtl No.} = 0.69$$

$$J = \text{mechanical equivalent of heat} = 778 \frac{\text{ft-lbf}}{\text{Btu}}$$

$$g = 32.2 \frac{\text{lbm-ft}}{\text{lbf-hr}}$$

The above numbers are for the case: H₂, $D = 0.500$, $p_{o2} = 250$ psia, $T_{o2} = 4000^\circ\text{R}$, $T_{o2} - T_{o1} = 2500^\circ\text{R}$. Upon substitution:

$$\frac{W}{Q} = 0.0042$$

$$Q = 500 \text{ Mw}_{th}$$

$$Q_f = 2.1 \text{ Mw pumping power}$$

This value of pumping power agrees fairly well with the pumping power estimate based on the average channel pressure drop, $\Delta p_{avg} \approx 8$ psia, $p_{o2} = 250$ psia, $p_{o1} = 258$ psia, for the above case using Eq. (29) which gives 3.53 Mw.

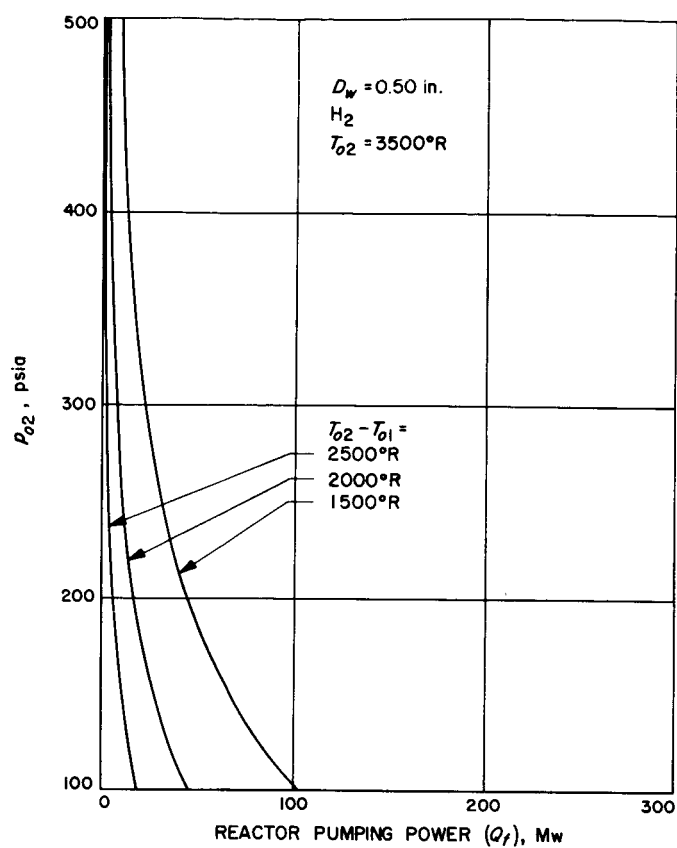
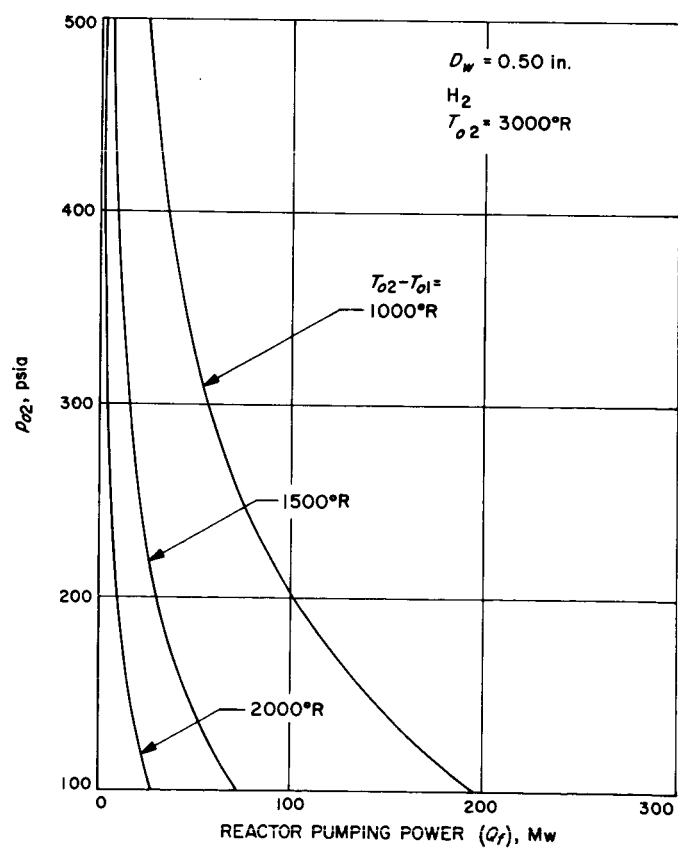


Fig. 10. Reactor pumping power parametric study at 3500°R, with H_2

Fig. 11. Reactor pumping power parametric study at 3000°R, with H_2



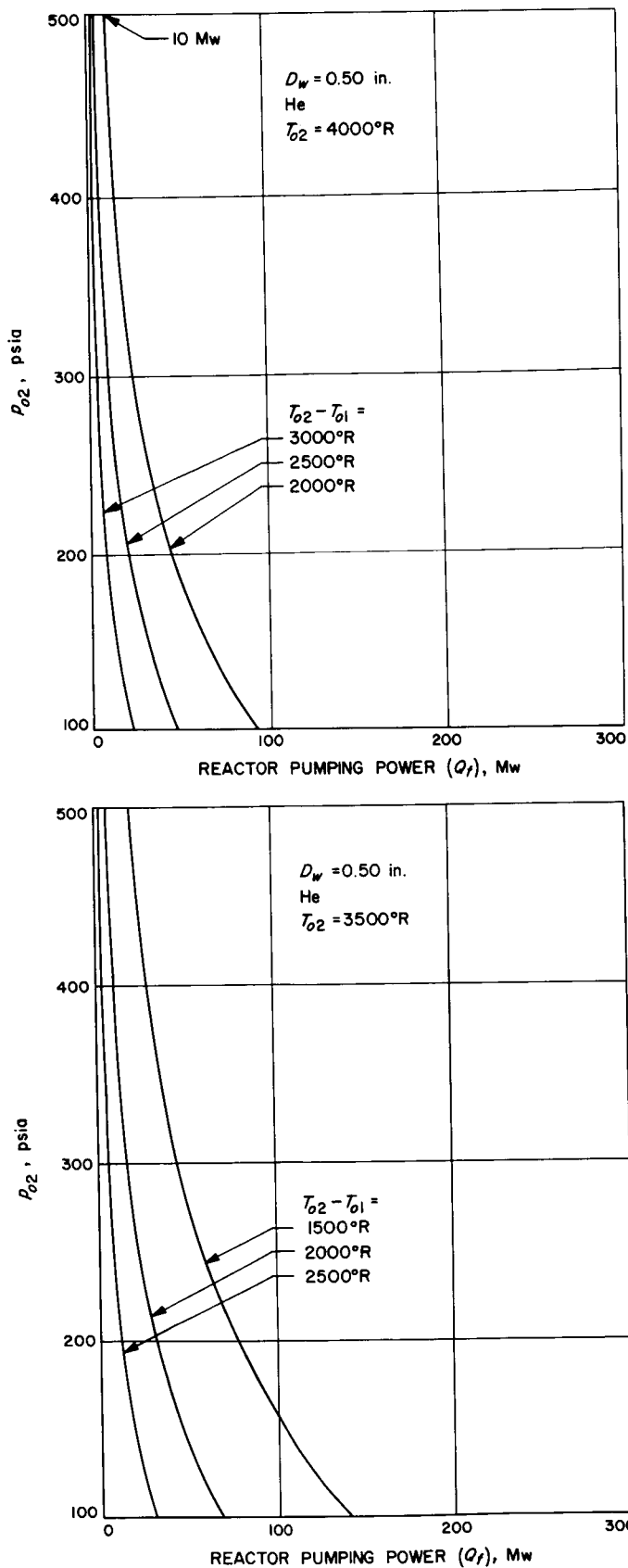


Fig. 12. Reactor pumping power parametric study at 4000°R, with He

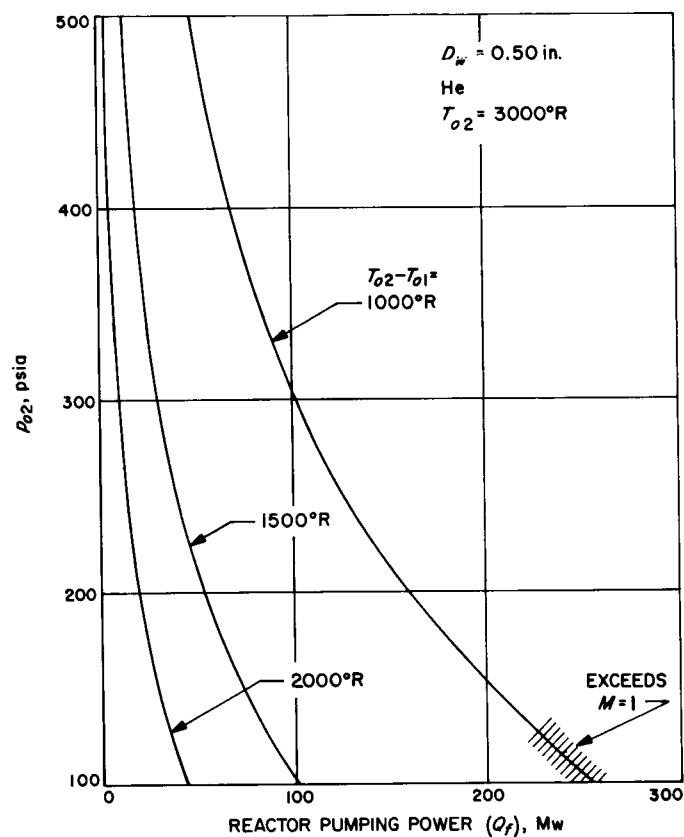
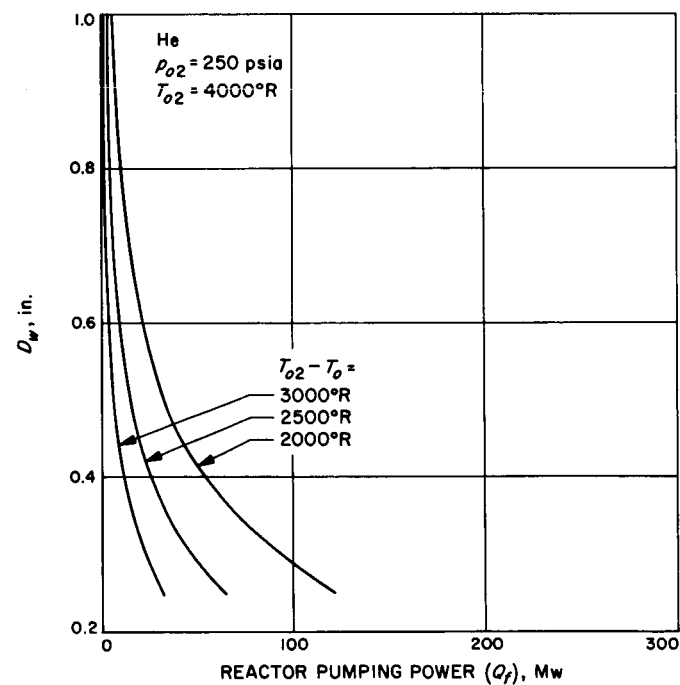
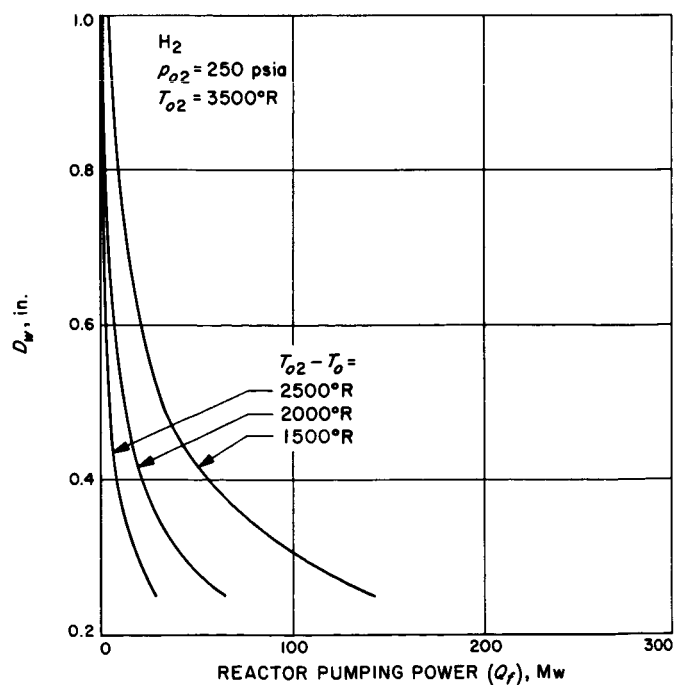
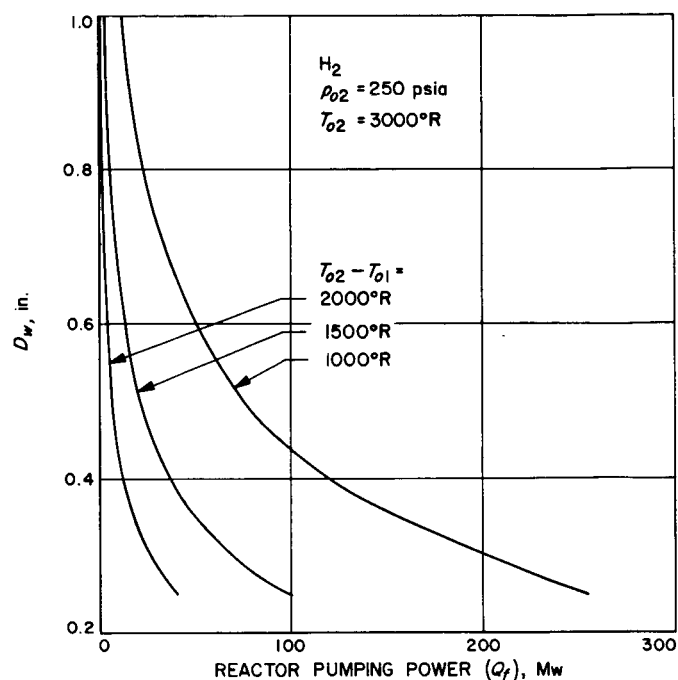
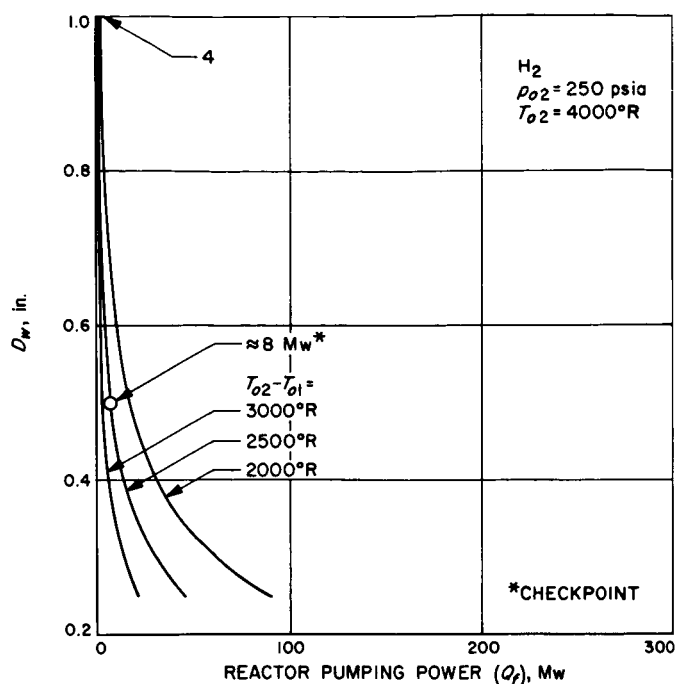


Fig. 14. Reactor pumping power parametric study at 3000°R, with He

Fig. 13. Reactor pumping power parametric study at 3500°R, with He



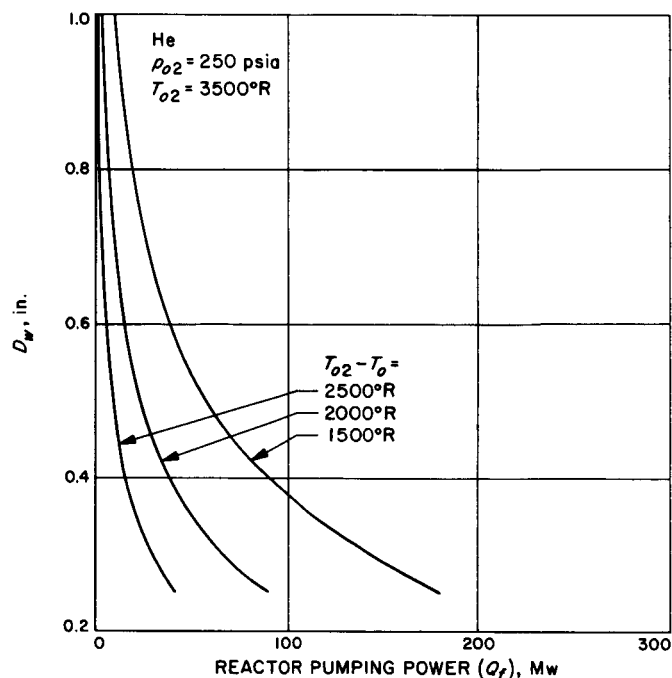


Fig. 19. Reactor pumping power parametric study at 3500°R and 250 psia, with He

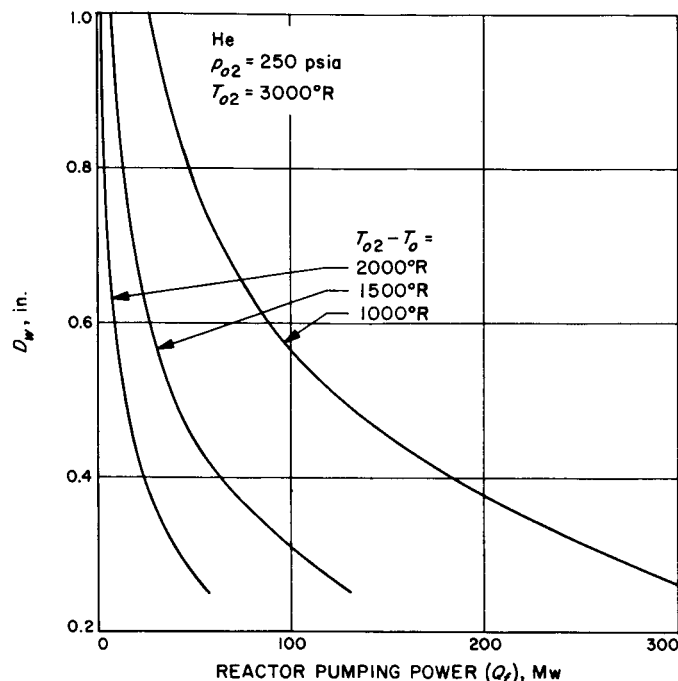


Fig. 20. Reactor pumping power parametric study at 3000°R and 250 psia, with He

III. TEMPERATURE DISTRIBUTION, PRESSURE DROP AND PUMPING POWER FOR THE SINGLE PHASE RADIATOR

A. Radiator Temperature Distribution

The fundamental problem here is to find the temperature distribution along a tube with hot gas flowing through it, and with radiation heat transfer to space on the outside surface. The basic tube material will be assumed to be graphite, although as explained later, a more logical tube structure would probably be a composite of refractory metal such as tungsten along with the graphite. The assumption for the present of all graphite tubes will not affect the subsequent calculations significantly since the temperature drop through the tube wall is small compared to the fluid film drop at the inside surface of the tube. Furthermore, the thermal conductivity of tungsten, rhenium, tantalum, molybdenum and niobium, the refractory metals, is greater than that of graphite so that

the tube surface temperatures arrived at will be less than what might be expected with a composite structure of graphite and any of the above metals. The tube outside diameter will again be taken to be $1\frac{1}{2} \times$ the tube inside diameter to ensure sufficiently low tube stresses at gas pressures up to 500 psia.

The radiator analysis will be restricted to consideration of only one gas, hydrogen, since this choice offers the lowest relative pumping power.

As an approximation, axial conduction of heat along the tube wall will be neglected. This should be a reasonable approach since the thermal conductivity of graphite is fairly low.

To simplify the present analysis, the entire tube outer surface is assumed to "see" an outer space temperature of 0°R . With an involute reflector scheme (described later) the view factor would actually be about 80%, and an allowance is made later on for this.¹³

The use of tube fins is not considered here, in deference to the involute reflector scheme mentioned above. Fins would not be as effective for the gas radiator as for the metal vapor condensing radiator. The condensing radiator suffers negligible temperature drop across the condensing fluid film and through the tube wall, hence, almost all of the thermal resistance is at the outside surface of the tube, and the overall effectiveness of the radiator can be greatly improved by extending the outside surface area through the use of fins. This is not the case with the gas radiator since much of the thermal resistance occurs at the inside surface of the tube due to the poorer heat transfer coefficient for gases.

An inlet gas temperature of 4000°R is assumed. This is based on an arbitrary desire to keep the maximum core temperature less than about 5000°R , but seems consistent with maximum gas temperatures being assumed in other gas-cooled reactor design concepts (such as Ref. 7) and with maximum gas temperatures actually achieved in recent experiments (such as Ref. 5). Furthermore the strength of refractory materials such as tungsten and graphite appears to be high enough up to 5000°R . In fact the tensile strength of graphite reaches a peak at about 5000°R (Ref. 12, Fig. 5-2).

The first problem is to determine the temperature distribution along a tube of unspecified length for an inlet

gas temperature of 4000°R and a reasonable mass flow rate. A tube ID of 0.500 in. is chosen for this case along with a mass flow rate of $\rho V = 19 \text{ lbm/ft}^2\text{-sec}$ which, according to the reactor analysis performed earlier, should give reasonable pressure drops. A point-by-point analysis was taken to be the simplest and most direct way of obtaining the desired result, Fig. 21. The applicable equations are:

$$q_{ow} = h A \Delta T = h \pi D_w \Delta x (T_o - T_w) \quad (32)$$

which, by applying Reynolds Analogy, Eq. (6), becomes:

$$q_{ow} = (\rho V) c_p \frac{f}{2} \left(\frac{1}{P_r} \right)^{0.6} \pi D_w \Delta x (T_o - T_w) \quad (33)$$

Also:

$$q_{ws} = \frac{2\pi \Delta x k}{\ln(r_s/r_w)} (T_w - T_s) \quad (34)$$

$$q_{so} = \pi D_s \Delta x \times 0.172 \left(\frac{T_s}{100} \right)^4 \quad (35)$$

The heat balance for flow in the tube is:

$$\begin{aligned} \frac{\pi}{4} D_w^2 (\rho V) c_p dT_o &= h \pi D_w dx (T_o - T_w) \\ dT_o &= 2f \left(\frac{1}{P_r} \right)^{0.6} \frac{dx}{D_w} (T_o - T_w) \end{aligned} \quad (36)$$

which in finite difference form becomes:

$$T_{om} - T_{o(m+1)} = 2f \left(\frac{1}{P_r} \right)^{0.6} \frac{\Delta x}{D_w} (T_o - T_w) \quad (37)$$

¹³Also, the effect of a tube surface emissivity of less than 1.0 was left out; however, for a graphite surface and many other surfaces, emissivities on the order of 0.95 can be expected so the error is not large.

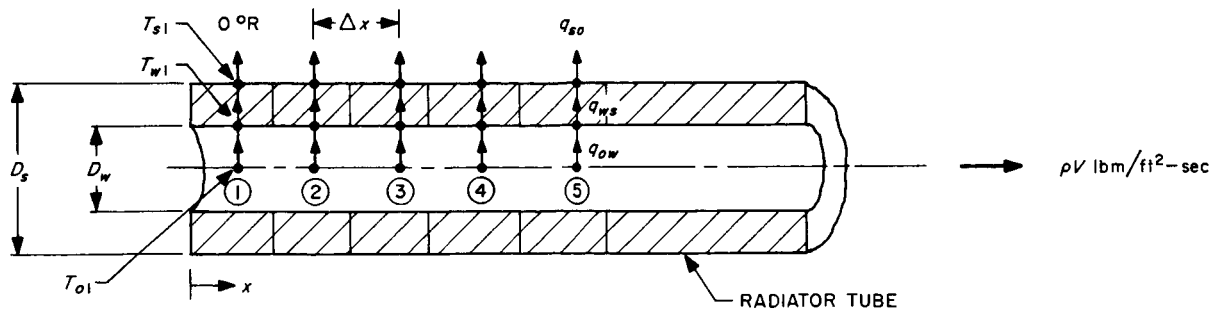


Fig. 21. Point-by-point thermal analysis of a radiator tube

It has been shown in the parametric study for the reactor that for the temperature ranges and Reynolds numbers of interest:

$$\left. \begin{aligned} c_p &= 3.6 \text{ Btu/lbm-}^\circ\text{R} \\ f &= 0.005 \\ \left(\frac{1}{P_r}\right)^{0.6} &= 1.25 \end{aligned} \right\} \text{ for H}_2$$

The increment of length Δx can be taken as 1.0 ft. Then Eq. (33-35) and (37) become:

$$q_{ow} = 127 (\rho V) D_w (T_o - T_w) \quad (38)$$

$$q_{ws} = \frac{k}{0.0645} (T_w - T_s) \quad (39)$$

$$q_{so} = 3.14 D_s \left[0.172 \left(\frac{T_s}{100} \right)^4 \right] \quad (40)$$

$$(T_{om} - T_{o(m+1)}) = 0.0125 \frac{(T_o - T_w)}{D_w} \quad (41)$$

Since for any station, $q_{ow} = q_{ws} = q_{so} = q$, Eq. (38-40) can be combined to give ($D_s/D_w = 1.5$):

$$\frac{T_o - T_s}{\left[\frac{371}{(\rho V)} + \frac{2025 D_s}{k} \right]} = \left[0.172 \left(\frac{T_s}{1000} \right)^4 \right] = F(T_s) \quad (42)$$

Eq. (42) can be used to find T_s for a known value of T_o for any station. Plot both sides of Eq. (42) to solve it graphically. The curves will cross at the appropriate value of T_s and $F(T_s)$. The value of k for any station is taken to be the value corresponding to T_o (this is conservative and introduces negligible error). As shown in Ref. 12, p. 142 (also Ref. 3, p. 23), the conductivity of graphite varies with temperature, can only be specified in a range of values at any specific temperature, and depends on whether the orientation of the heat flow is parallel or perpendicular to the extrusion axis of the graphite (parallel being the preferred orientation). For purposes of temperature distribution estimates, a median value of thermal conductivity will be used. (See median curve in Ref. 12,

p. 142.) Once T_s is known for a given station, T_o for the next station is found using Eq. (41) where:

$$\begin{aligned} T_o - T_w &= \frac{q}{127 (\rho V) D_w} \\ &= \frac{3.14 \times D_s}{127 (\rho V) D_w} F(T_s) \times 10^4 = \frac{371}{(\rho V)} F(T_s) \end{aligned} \quad (43)$$

So that

$$\Delta T_o = \frac{55.6 F(T_s)}{(\rho V) D_w} \begin{cases} \times 2 \text{ for } 2\Delta x \\ \times 3 \text{ for } 3\Delta x \end{cases} \quad (44)$$

(D_w in in.)

For $D_w = 0.500$ in., $T_{o1} = 4000^\circ\text{R}$, and $\rho V = 19$ lbm/ft²-sec, the above procedure was carried out and the result is plotted in Fig. 22; it can be seen that 80% of the radiator heat load in going from 4000 to 1500 $^\circ\text{R}$ in a 100-ft tube is disposed of in the first 50 ft. Therefore, for the particular geometry, temperatures and flow rate on which Fig. 21 is based, there would be considerable weight penalty for radiating below 2000 $^\circ\text{R}$.

In view of the above, the subsequent parametric analysis is based on fixed radiator inlet and outlet temperatures of 4000 and 2000 $^\circ\text{R}$, respectively. Furthermore, the lower temperature is felt to be about the maximum allowable blower temperature consistent with long life (10,000 hr) turbomachinery applications, and about the maximum allowable operating temperature for a cold boundary containment material such as Inconel or stainless steel (hot boundary envisaged as being contained by a pressure envelope of cooler gas — see Section IV).

B. Radiator Size

The procedure outlined above was repeated for the following combinations of D_w and ρV to find the required tube length and temperature distributions for $T_{o1} = 4000^\circ\text{R}$ and $T_{o2} = 1950^\circ\text{R}$ (50 $^\circ\text{R}$ allowance for temperature rise in the compressor):

D_w , in.	D_s , in.	ρV	lbm/ft ² -sec
0.25	0.375	$\rho V = 15, 30, 50$	
0.50	0.750	$\rho V = 6, 12, 24, 48$	
0.75	1.125	$\rho V = 4, 8, 16, 32$	

The tube lengths for each case are given in Table 9, along with the required number of tubes to dispose of 500 Mw, and relative size and weight tabulations.

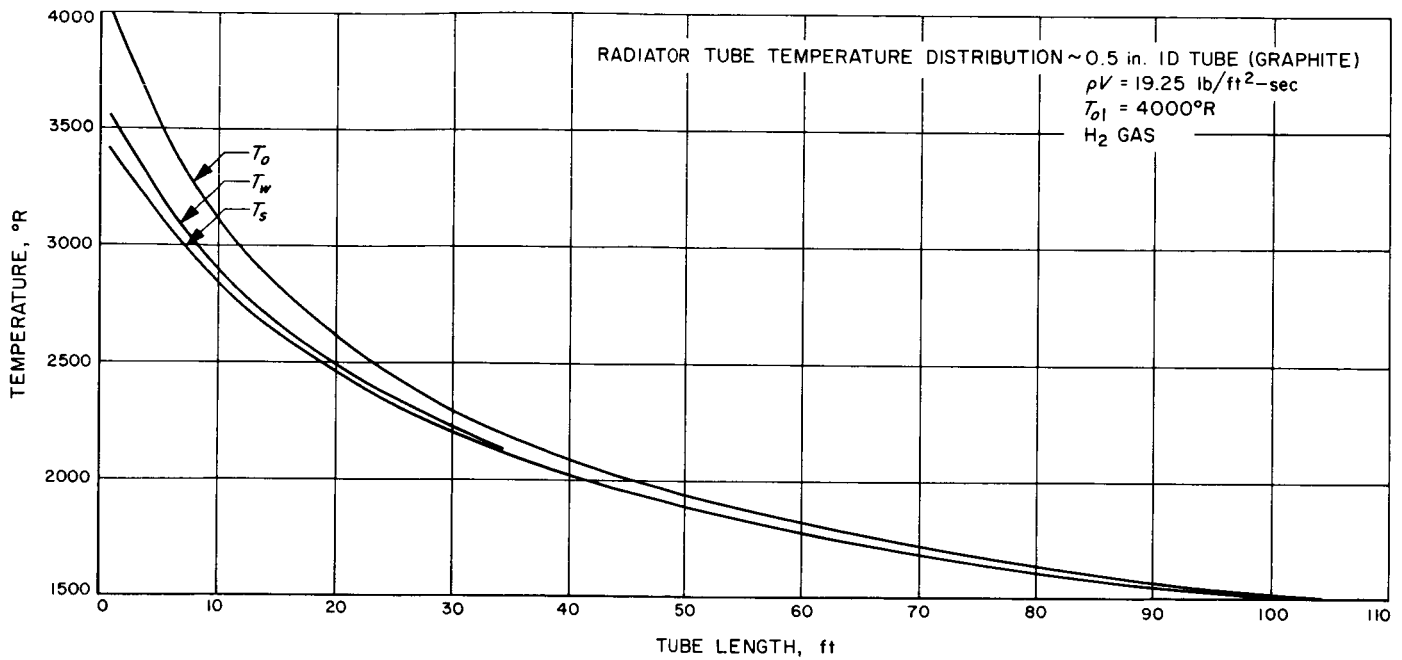


Fig. 22. Radiator tube temperature distributions

Table 9. Radiator thermal parametric analysis results

D_w , in.	(D_s) , in.	ρV , lbm/ft ² -sec	L , ft	L/D_w	N , tubes	Relative size and weight	
						Size	Weight
						$N \times \left(\frac{D_s}{12}\right) \times L$, ft ²	$9000 \left(\frac{L}{\rho V}\right)$, lb
0.25	(0.375)	15	18.65	74.6	12,843	7,485	11,200
		30	34.57	138	6,422	6,938	10,350
		60	65.56	262	3,211	6,579	9,810
0.500	(0.750)	6	19.60	39	8,027	9,833	29,430
		12	32.59	65.2	4,013	8,174	24,480
		24	58.50	117	2,007	7,338	21,960
0.750	(1.125)	48	107.74	215	1,003	6,754	20,160
		4	22.99	30.5	5,334	11,496	51,750
		8	36.61	48.8	2,667	9,154	41,220
		16	63.20	24.3	1,333	7,898	32,550
		32	114.57	153	667	7,164	32,220

$$N = \frac{\text{Total mass flow rate}}{(\rho V) \times \text{total tube area}} = \frac{W}{(\rho V) A_t}$$

$$W = \frac{500 \text{ Mw} \times 3.413 \times 10^6 \text{ Btu/hr} - \text{Mw}}{3.6 \text{ Btu/lbm-}^\circ\text{R} \times (4000 - 2000) \times 3600} = 65.5 \text{ lbm/sec}$$

$$\text{Weight} = N \frac{\pi}{4} (D_s^2 - D_w^2) L \rho = N A_t \times 1.25 L \rho$$

$$\rho \text{ (for graphite)} = 110 \text{ lbm/ft}^3$$

$$= L \frac{65.5}{(\rho V)} 1.25 \times 110$$

$$= 9000 \frac{L}{\rho V}$$

The information in Table 9 is plotted in Fig. 23 and 24, which show clearly the size and weight advantage in going to small diameter tubes. This is to be expected because of the greater surface to flow area ratio for smaller tubes, and also because the tube walls can be made thinner for a given internal pressure.

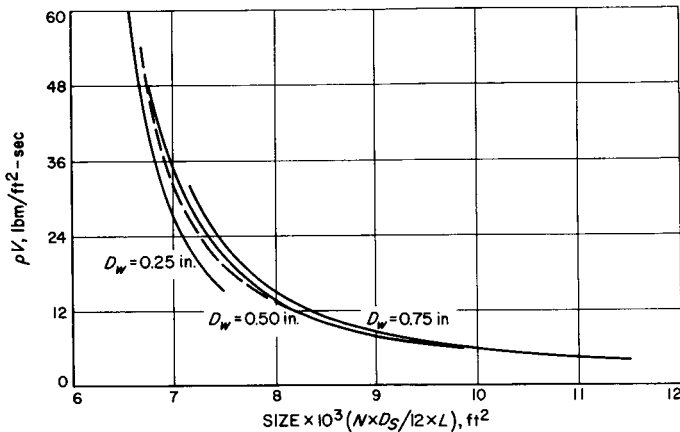


Fig. 23. Radiator relative size variation vs mass flux (ρV)

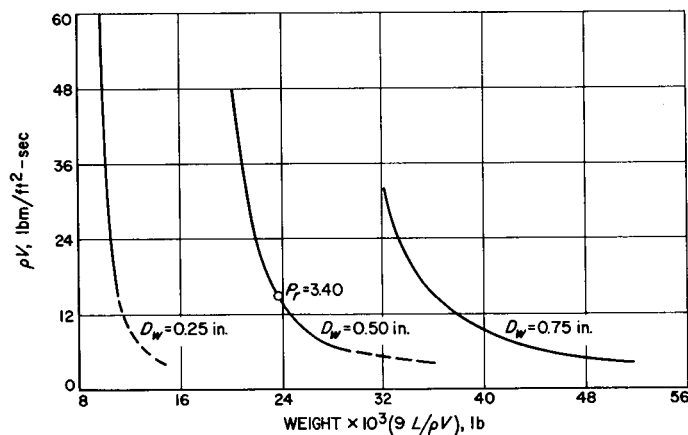


Fig. 24. Radiator relative weight variation vs mass flux (ρV)

It should be noted that the length to diameter ratio L/D_w is independent of D_w for a given value of ρV . This is shown in Fig. 25. This is a very interesting correlation. It shows that a given value of ρV fixes the tube surface area required for a specified temperature drop. It is also a convenient correlation since it precludes the necessity

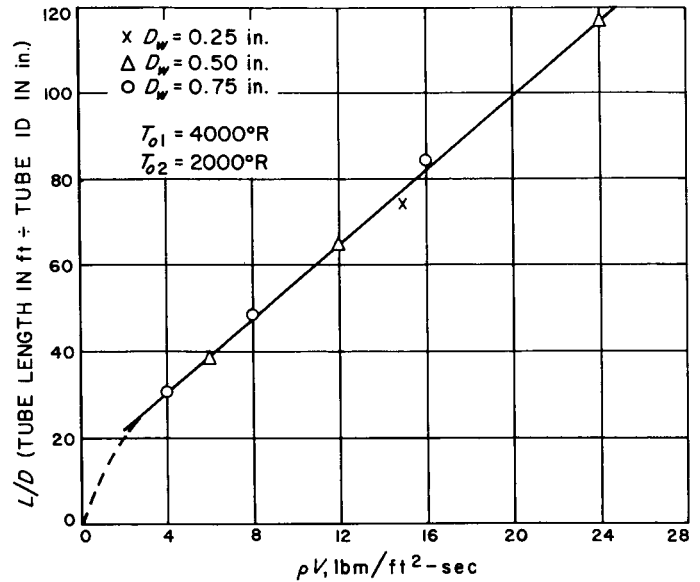


Fig. 25. Relationship between length/diameter ratio (L/R) and mass flux (ρV), radiator tubes

of repeating the tedious graphical analysis carried out in this section for other values of ρV and D_w .¹⁴

C. Radiator Pressure Drop and Pumping Power

Eq. (14) can be used to calculate the pressure ratio across a radiator tube since it applies to both heating and cooling:

$$1 - \left(\frac{P_{o2}}{P_{o1}} \right)^2 = \gamma M_i^2 B_1 \mathcal{Q}_1 \left(4f \frac{L}{(D_w/12)} \right) \quad (45)$$

$$\begin{aligned} \mathcal{Q}_1 &= \int_0^1 \frac{T_o}{T_{o1}} \left[\frac{1}{2} \frac{T_w - T_o}{T_o} \left(\frac{1}{P_r} \right)^{0.6} + 1 \right] d \left(\frac{x}{L} \right) \\ &= \int_0^1 \frac{T_o}{T_{o1}} \left[1 - \frac{1}{2} \frac{T_o - T_w}{T_o} \left(\frac{1}{P_r} \right)^{0.6} \right] d \left(\frac{x}{L} \right) \end{aligned} \quad (46)$$

It was found that B_1 as given by Eq. (15) was very close to 1.0 for the cases of interest (i.e., low pumping power).

It should be noted that since $T_o > T_w$ for cooling, \mathcal{Q}_1 is a much smaller number than if $T_w > T_o$ which would be the case for heating. This has the effect of increasing p_{o2}/p_{o1} closer to 1.0, which means a lower Δp and lower pumping power for cooling than for heating. This effect

¹⁴Furthermore, it is apparent that the problem could have been solved analytically for the general case of any gas radiator in terms of $T_{o1} - T_{o2}$ and the coolant gas parameters. This should be done at some later time.

Table 10. Radiator hydraulic parametric analysis results

D _w , in.	ρV	$4f \left[\frac{L}{(D_w/12)} \right]$	Q ₁	p _{o1} = 480 psia					p _{o1} = 380 psia					p _{o1} = 280 psia				
				M ₁	$1 - \left(\frac{p_{o2}}{p_{o1}} \right)^2$	$\frac{p_{o2}}{p_{o1}}$	Δp _o , psia	Q ₁ , Mw	M ₁	$1 - \left(\frac{p_{o2}}{p_{o1}} \right)^2$	$\frac{p_{o2}}{p_{o1}}$	Δp _o	Q ₁	M ₁	$1 - \left(\frac{p_{o2}}{p_{o1}} \right)^2$	$\frac{p_{o2}}{p_{o1}}$	Δp _o	Q ₁
0.25	15	17.93	0.6107	0.0567	0.0493	0.9750	12.00	3.535	0.0716	0.0786	0.9599	15.24	5.69	0.0972	0.1448	0.9248	21.05	10.85
	30	33.24	0.6232	0.1134	0.3729	0.7919	99.89	31.72	0.1433	0.5955	0.6360	138	59.6	0.1945	1.0971	—	—	—
	60	63.04	0.6281	0.2269	2.8539	—	—	—	0.2866	4.5533	—	—	—	0.3889	8.384	—	—	—
0.50	6	9.40	0.6077	0.0227	0.00412	0.9979	1.008	0.2946	0.0287	0.00659	0.9967	1.254	0.442	0.0389	0.0121	0.9939	1.708	0.835
	12	15.63	0.6183	0.0454	0.0279	0.9860	6.720	1.9640	0.0573	0.0444	0.9775	8.55	3.19	0.0778	0.0819	0.9582	11.704	5.94
	24	28.06	0.6265	0.0908	0.2029	0.8928	51.456	15.663	0.1146	0.3232	0.8227	67.4	26.7	0.1556	0.5959	0.6357	102	59
	48	51.67	0.6319	0.1815	1.5058	—	—	—	0.2293	2.4034	—	—	—	0.3111	4.42	—	—	—
0.75	4	7.36	0.5989	0.0151	0.00141	0.9993	0.336	0.0982	0.0191	0.00225	0.9989	0.418	0.147	0.0259	0.0041	0.9979	0.588	0.2946
	8	11.72	0.6147	0.0302	0.00920	0.9954	2.208	0.6383	0.0382	0.0147	0.9926	2.81	1.03	0.0519	0.0272	0.9863	3.836	1.92
	16	20.22	0.6251	0.0605	0.0648	0.9671	15.792	4.665	0.0764	0.1033	0.9469	20.2	7.61	0.1037	0.1903	0.8998	28	14.6
	32	36.66	0.6319	0.1210	0.4748	0.7247	131.664	43.21	0.1528	0.7572	0.4927	193	90	0.2074	1.395	—	—	—

is consistent with observed results, Ref. 13. It would then be expected that the pumping power might be lower for the radiator than for the reactor. This possibility is further enhanced by the absence of peaking factors in the radiator and the consequent uniformity of heat load for all tubes.

\mathcal{D}_1 was found by graphically integrating the temperature distributions found in the previous section over the length of the tube. As might be expected from the non-dimensionalized form of Eq. (46) and the similarity of temperature, $T_{o1} - T_{o2} = 2000^\circ\text{R}$ for all cases. \mathcal{D}_1 is about the same (≈ 0.62), for all combinations of ρV and D_w .

Using $f = 0.005$ and $P_r = 0.69$ (for H_2), the pressure ratios were calculated from Eq. (45) where, as in Eq. (20):

$$M_1 = \frac{\rho V}{p_{o1}} \left(\frac{RT_{o1}}{\gamma g_c} \right)^{1/2} = 1.815 \frac{(\rho V)}{p_{o1}} \quad (47)$$

(p_{o1} in psia)

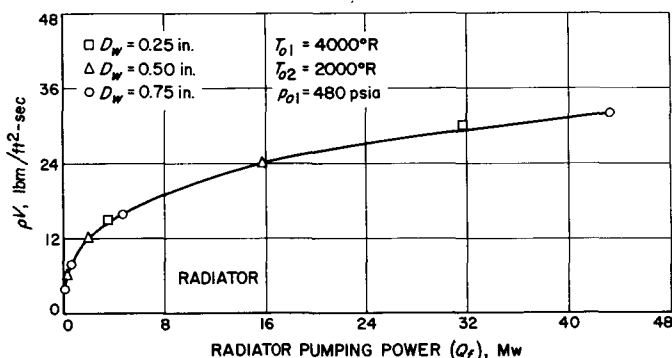


Fig. 26. Radiator pumping power as a function of mass flux (ρV), $p_{o1} = 480$ psia

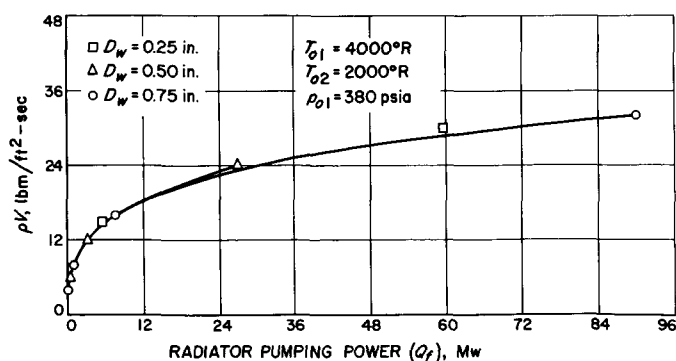


Fig. 27. Radiator pumping power as a function of mass flux (ρV), $p_{o1} = 380$ psia

The results are listed in Table 10 along with the estimate of pumping power, which, similar to Eq. (29), can be written:

$$Q_f = W c_p T_{out} \left[1 - \left(\frac{p_{in}}{p_{out}} \right)^{\gamma-1/\gamma} \right] \quad (48)$$

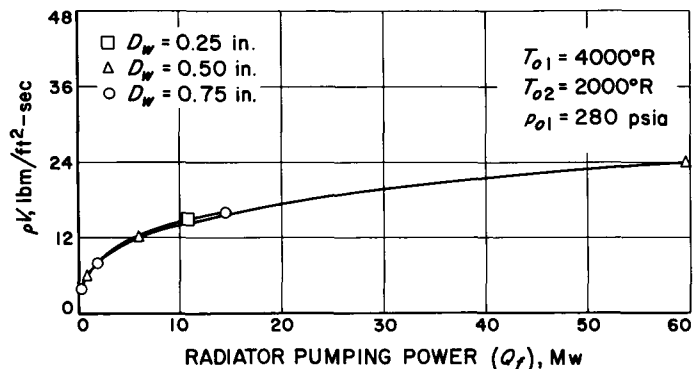


Fig. 28. Radiator pumping power as a function of mass flux (ρV), $p_{o1} = 280$ psia

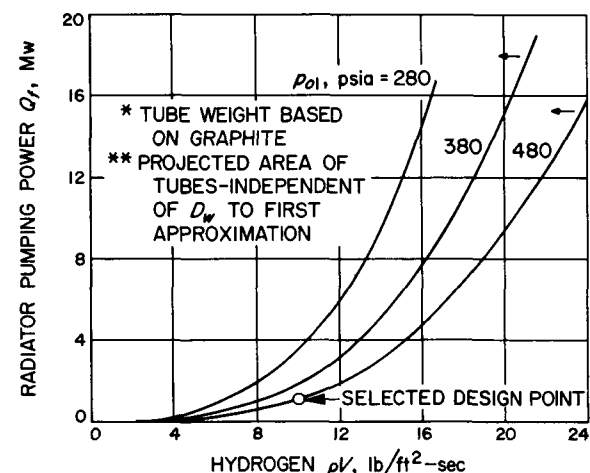
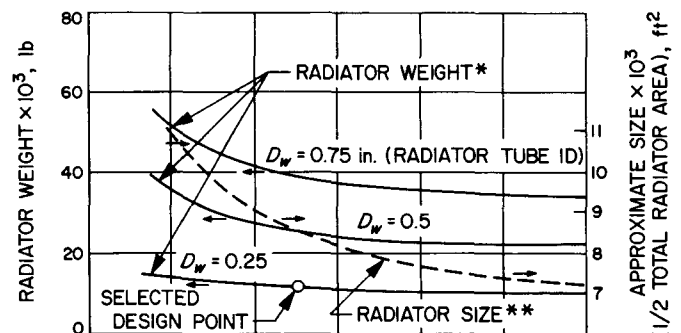


Fig. 29. Summary of radiator parametric analysis

where

p_{in} = compressor inlet pressure ($=p_{o2}$ for the radiator)

p_{out} = compressor outlet pressure ($=p_{o1}$ for the radiator)

T_{out} = compressor outlet temperature

T_{out} is taken to be 2000°R reactor inlet temperature less 25°R allowance for temperature rise in the compressor stages required to overcome the reactor pressure drop or $T_{out} = 1975^{\circ}\text{R}$. Substituting, $W = 65.5 \text{ lbm/sec}$:

$$Q_I = 491 \left(1 - \frac{p_{o2}}{p_{o1}} \right)^{0.286} \quad (49)$$

The results of Table 10 are plotted in Fig. 26-28 for $p_{o1} = 480, 380$ and 280 psia , respectively. Radiator pumping power is expressed as a function of mass flux, ρV ($\text{lbm/ft}^2\text{-sec}$). It is interesting that the pumping power is apparently independent of the tube diameter D_w . This is a consequence of Eq. (45) and the fact that L/D_w is a function only of ρV and not D_w as shown in Fig. 25, and

that \mathcal{D}_1 comes out to be approximately the same for all values of D_w as explained earlier.

For clarity, the results of Fig. 23 and 24, and 26-28 are condensed into one graph, Fig. 29. It is clear that for minimum weight the radiator tube diameter should be as small as practicable. Fig. 29 also shows the effect of operating pressure and ρV on pumping power. It is clear that ρV should be 10 to 12 $\text{lbm/ft}^2\text{-sec}$ or less in order to keep pumping power down to reasonable values. As expected, the pumping power for the radiator could be made substantially less than that for the reactor.

For values of ρV of less than 10, the radiator size grows disproportionately to the savings in pumping power. This is due to the rapid increase in the number of tubes required for lower values of ρV (see Table 9).

For the reasons stated above, $D_w = 0.25 \text{ in.}$ and $\rho V = 10 \text{ lbm/ft}^2\text{-sec}$ are chosen as the reference parameters for the suggested radiator configuration in Section VI. From Fig. 25, $\rho V = 10$ corresponds to a tube length of 14 ft.

IV. SUGGESTED PLANT DESIGN CONCEPT

In order to obtain a realistic estimate of the weight of a gas-cooled fission-electric reactor power plant, it is necessary first to envisage some practical or at least hopeful design and arrangement for such a plant. This is the purpose of this brief section.

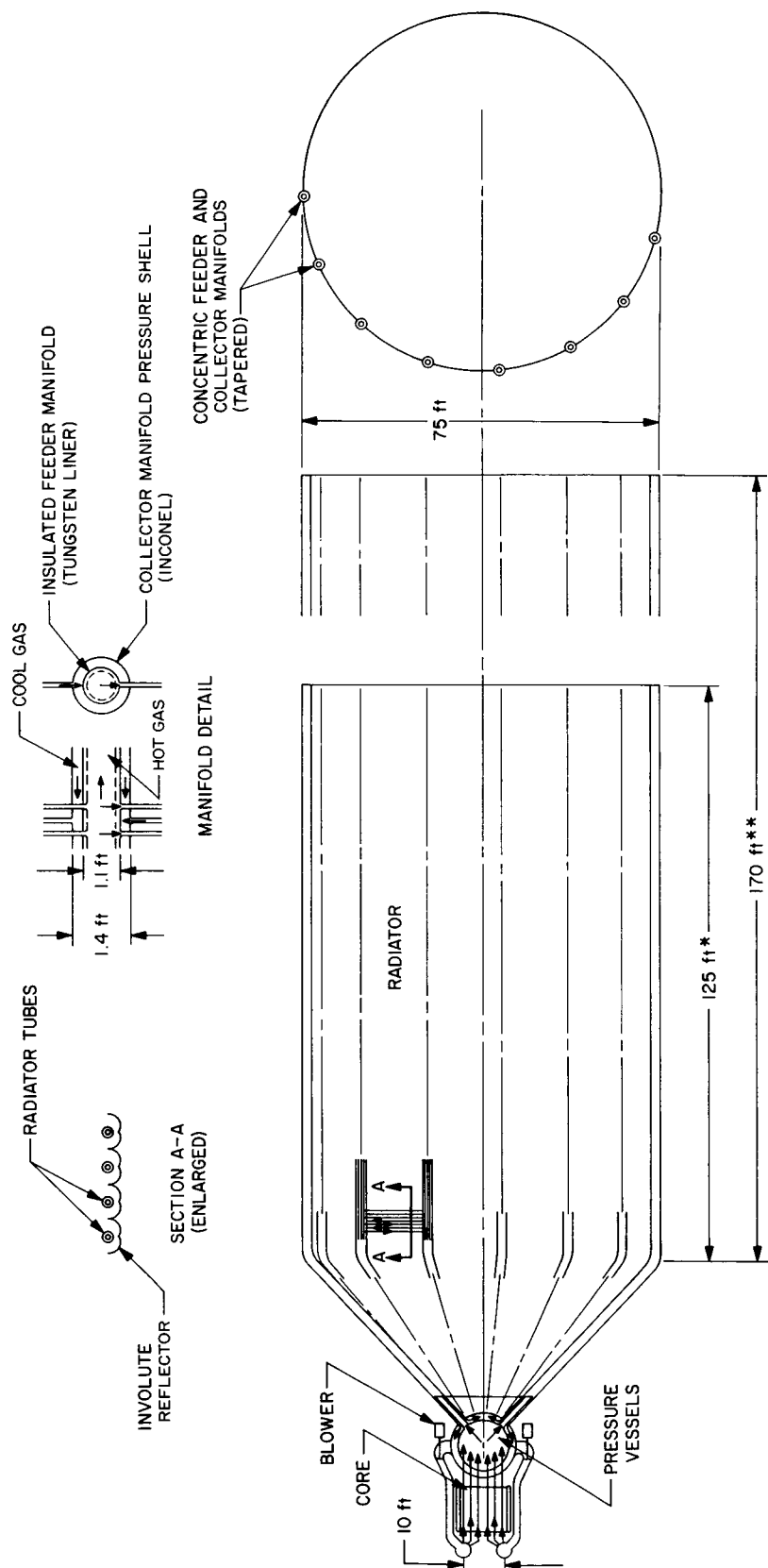
Given the number of tubes necessary to dispose of 500 Mw of thermal energy in a gas radiator, the lightest possible scheme would seem to be a flat radiator which could radiate from both sides. However, this is not a practical idea from the standpoint of launch limitations; and it presents the problem of ducting the hot reactor outlet gas to the extremities of such a radiator and back again to the reactor inlet. A more practical radiator shape would be either conical, cylindrical, or a combination of the two.

There is a considerable problem involved in containment of the very hot gas at high pressure. The long term creep strength of even the refractory metals is on the

order of a few thousand pounds per square inch at the peak gas temperatures considered here; and in addition there is the problem of diffusion of hot gases through solids at high temperatures (see for example Ref. 11). It would seem necessary to resort to concentric pressure vessels and feeder manifolds to reduce the pressure differential across the hot gas pressure boundaries in order to keep the hot boundary stresses acceptably low and to reduce the gas diffusion rate through the hot boundary.

The mechanical complexity inherent in the variety of access channels¹⁵ that must be provided in at least one end of a fission-electric reactor has been discussed in Section II-A. It was pointed out that the needs for access to these channels would favor a pressure tube core concept as opposed to a reactor completely enclosed in a pressure vessel.

¹⁵I.e., vacuum channels, fission cell coolant channels, driver channels, control rods.



25 Mw_e GAS COOLED FISSION ELECTRIC REACTOR AND RADIATOR CONCEPT
(ASSUMING 5% FISSION-ELECTRIC CONVERSION EFFICIENCY)***

* BASED ON 0.375 in. OD RADIATOR TUBE
** BASED ON 0.500 in. OD RADIATOR TUBE
*** FOR 10% CONVERSION EFFICIENCY THE RADIATOR AREA
REQUIRED WOULD BE APPROXIMATELY HALF OF THE AREA
SHOWN IN THE ABOVE SKETCH—AND WOULD BE EQUIVALENT
TO A CYLINDER 60 ft IN DIAMETER BY 100 ft IN LENGTH

Fig. 30. Gas-cooled fission-electric reactor and radiator concept

The above considerations were factored into the design and arrangement concept shown in Fig. 30. The pressure tubes which penetrate the core are brought together in a common plenum in the shape of a spherical vessel from which hot gas feeder manifolds branch out to the radiator. The hot gas enclosures would consist of insulated tungsten liners surrounded by a pressure envelope of relatively cool gas returning from the radiator. The radiator tubes are supplied from the inner annulus of the manifolds. The tube outlets are discharged into the outer annulus. The pressure differential across the hot gas boundary would then be about equal to the pressure drop through the radiator tubes, only a few psi. The radiator tubes themselves are small enough that the wall thickness required to keep the tube stresses very low is reasonable ($D_s = 1.5 D_w$). As pointed out earlier, this wall thickness might also suffice for meteoroid protection.

The length of the radiator tubes shown in Fig. 30 (≈ 14 ft) is approximately the length of 0.25-in. ID tube necessary to reduce the gas temperature from 4000°R for $\rho V = 10 \text{ lbm/ft}^2\text{-sec}$. $D_w = 0.25$ in. and $\rho V = 10$ are the chosen reference parameters based on the analysis of the previous section (see Table 9, Fig. 25 and 29). Each tube is provided with an involute reflector as shown in Fig. 31, which is taken from ORNL-LR-DWG 3727.¹⁶ The involute profile is generated by unwinding a "string" which is wrapped around the outside surface of the tube starting at point 0. Every point of the involute surface is then at right angles to a line drawn tangent to the tube surface. The width of the reflector is equal to the circumference of the tube, so that, in effect, the hot outside surface of the tube is unwrapped and projected outward toward space. Clearly, if the radiation from the surfaces of the tube and the reflector is emitted in a direction nor-

mal to the tube surface, then all of the rays are reflected away from the tube surface and the efficiency of the reflection could approach 100%. On the other hand, if the reflection is completely diffuse, some of the radiation is reflected back to the tube surface and the reflector efficiency is reduced. For purposes of constructing Fig. 30, it was assumed that the reflector effectiveness would be about 80%. (Most cases of heat radiation from surfaces are not normal and not completely diffuse—see for example Ref. 16.) The area of the cylindrical portion of the radiator shown in Fig. 30 was set equal to $N\pi D_s L$ where L is the tube length and N the number of tubes required to radiate 500 Mw of heat energy for 100% reflector effectiveness. (For $D_w = 0.25$ in. and $\rho V = 10$, $N = 19,300$ tubes. See Table 9 and Section IV-4.) The area of the conical portion of the radiator is approximately 20% of the total surface, which compensates for the reduced reflector effectiveness.

The radiator manifolds are tapered as shown in Fig. 30, and are sized to give a normal gas velocity of about 200 ft/sec for the gas flowing to and from the radiator at a nominal pressure of 500 psia. For 15 headers, as shown in Fig. 30, the hot manifold diameter (at the large end) would then have to be about 1.1 ft, and the "cold" manifold diameter about 1.4 ft. A gas velocity of 200 ft/sec is equivalent to a hot gas Mach number of 0.017. This is only a fraction of the Mach number magnitude in the core and the radiator tubes and should result in a small pressure drop through the manifolds as compared with the core and radiator pressure drops.

In summary, the design concept suggested in Fig. 30 might provide one means for handling very high temperature reactor outlet gas and the subsequent weight estimates are based upon it. It also leaves space at the reactor inlet for venting of the reactor vacuum channels and for bringing in separate coolant channels for the driver fuel modules.¹⁷

The concept suggested in Fig. 30 is not without problems. There is of course the question of coolant gas loss by diffusion through material boundaries. In addition, thermal stress problems involved with hot tubes penetrating relatively cool pressure boundaries could be severe, and this is further complicated by the number of such penetrations which would be required. There is also the problem that the penetration seals would probably consist of bimetallic welded joints, possibly between a

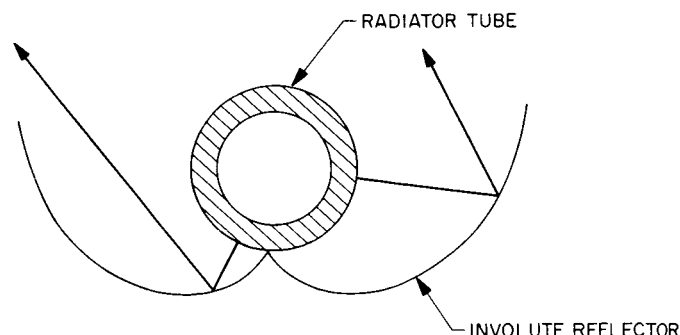


Fig. 31. The involute reflector

¹⁶ORNL-LR-DWG 3727, Schematic Diagram of an Involute Reflector.

¹⁷The driver coolant could enter and leave the reactor at the same end of the core, i.e., a two-pass scheme.

tungsten alloy and perhaps Inconel. All of this raises the question of whether a radiator of the type and size shown in Fig. 30 would even be feasible. For purposes of ob-

taining a weight estimate, however, the concept was considered to be representative of the size and weight that one might expect for such a radiator.

V. WEIGHT ESTIMATE—GAS-CYCLE COMPONENTS

A. Reactor Core Weight

The weight of the reactor core, consisting of graphite moderator and refractory metal pressure tubes, is calculated as follows:

$$754 \text{ ft}^3 \times 0.50 \text{ solid fraction} = 377 \text{ ft}^3 \text{ solid volume}$$

$$\text{Specific gravity of graphite} \approx 1.75$$

$$\begin{aligned} \text{Graphite density } 1.75 \times 62.4 &= 109 \text{ lb/ft}^3 \\ &\times 377 = 41,000 \text{ lb} \end{aligned}$$

For purposes of estimating weight, pressure tubes are 0.50 in. ID. It is probable that tubes of some refractory metal such as Tungsten (W) or Rhenium (Rh) could be required to carry the coolant through the core and into the spherical hot gas reservoir.

$$\left. \begin{array}{l} \text{Specific gravity of W} = 19.1 \\ \text{Specific gravity of Rh} = 20.5 \end{array} \right\} \text{Approximately } 20$$

A tube wall thickness allowance of 0.0625 in. ($\frac{1}{16}$ in.) should be adequate on the average since, by itself, such a tube would be subjected to a hoop stress at 500 psia internal pressure of:

$$\sigma_H = \frac{p D_w}{2t} = \frac{500 \text{ in.} \times 0.50 \text{ in.}}{2 \times 0.0625} = 2000 \text{ psi}$$

$$\text{wt/ft} = \pi \frac{0.50}{12} \times \frac{0.0625}{12} \times 20 \times 62.4 = 0.85 \text{ lb/ft}$$

Needed: $3500 \text{ tubes} \times \approx 12 \text{ ft length each} = 42,000 \text{ ft} \times 0.85 = 35,800 \text{ lb}$. Total reactor weight = 76,800 lb

B. Reflector Weight

The weight of the reflector, 6-in. thick graphite assumed, is calculated as follows:

$$\frac{\pi}{4} (10.5^2 - 10^2) \times 10 = 102 \text{ ft}^3 \times 109 \text{ lb/ft}^3 = 11,150 \text{ lb}$$

C. Spherical Pressure Vessels

The weight of the concentric spherical pressure vessels which feed the reactor and the radiator are calculated as follows:

Take 12-ft diameter inner vessel, 14-ft diameter outer vessel,

Assume a shell of Inconel X.

(Stress for 1% creep in 10,000 hr @ 1800°R = 35,000 psi (Ref. 12, p. 154);

Take allowable stress of 25,000 psi

$$\sigma_H = \frac{p \times \frac{\pi D^2}{4}}{\pi D \times t_1} = 25,000 \text{ psi}$$

for $D = 14 \text{ ft}$ and $p = 500 \text{ psia} \rightarrow t_1 = 0.84 \text{ in.}$

Assuming the 0.84-in. thick outer vessel and a $\frac{1}{16}$ -in. thick inner liner of tungsten, the weight of the spherical pressure vessels, together with appropriate nozzles and fifteen 4-ft feeder stubs to the radiator manifolds, comes out to be about 33,200 lb.

D. Reactor Inlet Manifold and Manifold Feeder Pipes

A weight analysis indicates that these items would weigh approximately 7,700 lb.

E. Radiator Area

The radiator weight estimates in subsection F, following, are based on this radiator data:

From Table 9

$$N = \frac{W}{(\rho V) A_t} (\text{number of tubes})$$

$$\left. \begin{aligned} W &= 65.6 \text{ lb/sec} \\ (\rho V) &= 10 \text{ lb/ft}^2\text{-sec} \\ A_t &= 0.00034 \text{ ft}^2 (D_w = 0.25 \text{ in.}) \end{aligned} \right\} \rightarrow N = 19,300 \text{ tubes}$$

$$\pi D_s = \pi \frac{0.375 \text{ in.}}{12} = 0.098 \text{ ft} = \text{reflector width}$$

$$\text{Radiator length} = L_R = \frac{19,300}{15} \times 0.098 = 126 \text{ ft}$$

Radiator circumference:

$$\text{Tube length} = 14 \text{ ft (Fig. 23)}$$

$$\text{Manifold OD (max} = 1.4 \text{ ft} \times 15 = 21 \text{ ft)}$$

$$\text{Circumference} = 15 \times 14 + 21 = 231 \text{ ft}$$

$$\pi D_R = 231 \text{ ft}$$

$$D_R = 73.6 \text{ ft (Use 75 ft)}$$

$$\text{Radiator area (Cylindrical portion)} = 231 \times 126 = 29,100 \text{ ft}^2$$

Radiator area (Conical portion):

$$\text{Area of cone} = 2\pi rh$$

Area of truncated 45-deg cone is:

$$\begin{aligned} A &= 2\pi (r_1^2 - r_2^2) \\ &= 2\pi (37.5^2 - 10^2) = 8,160 \text{ ft}^2 \\ &\text{or } > 20\% \text{ of total area} \end{aligned}$$

F. Radiator Weight

1. Manifold Weight

For purposes of weight estimate, the manifolds were sized for a nominal gas velocity of 200 ft/sec. This gas velocity, together with the total mass flow rate of 65.6 lbm/sec through the radiator result in a total of 14.05 ft² of hot manifold inlet area and 7.0 ft² of cold manifold exit area. These areas, divided among 15 manifolds require a maximum outer manifold diameter of 1.335 ft and a maximum inner manifold diameter of 1.10 ft. The manifold can be tapered since the volume flow rate diminishes approximately linearly along the lengths of the manifolds.

Assuming an allowable stress of 25,000 psi for an Inconel outer manifold pipe, and a tapering wall thickness, the total weight for the outer manifolds comes out to be 26,250 lb.

For a constant-thickness inner manifold of tungsten (assume 0.030-in. thickness is adequate) the total weight for the inner manifolds would be about 13,250 lb.

2. Radiator Tube Weight

Assume thin tungsten liner of 0.010 in. with 0.100 in. graphite outer shell. (Then $D_s \approx 2.0 D_w$. This is inconsistent with the assumed diameter ratio of $D_s/D_w = 1.5$ taken for the calculation of temperature distribution and tube length. However, since the major portion of the temperature drop is through the gas film at the tube surface the error should not be large. Also, for $D_s \approx 2.0 D_w$ the radiator area is increased as shown in Fig. 30. It was felt that a 0.050-in. graphite layer for $D_s \times 1.5 D_w$ would be too thin.)

$$19,500 \text{ tubes} \times 14\text{-ft tube length} = 273,000 \text{ ft of tube}$$

$$\text{Total tungsten weight, radiator tubes} = 17,800 \text{ lb}$$

$$\text{Total graphite weight, radiator tubes} = 33,350 \text{ lb}$$

$$\frac{W_t}{\text{Area}} = \frac{35,350 \text{ lb}}{29,100 \text{ ft}^2} = 1.22 \text{ lb/ft}^2$$

$$\text{Conical area} = 8,160 \text{ ft}^2 \times 1.22 = 9,930 \text{ lb}$$

$$\text{Total radiator tube weight} = 45,280 \text{ lb}$$

3. Involute Reflector Weight

Assuming that the reflector can be made very thin (e.g., 0.015 in.) and that it can be made of Titanium (sp. gr. = 4.64) the weight of the reflector, including the conical area, would be about 26,050 lb.

4. Gas Cycle Radiator Total Weight

Based on the preceding estimates, the total weight for the gas cycle radiator is summarized as:

Manifolds	39,500 lb
Tubes	45,280 lb
Reflector	26,050
	<hr/> 110,830

Structural allowance $\times 1.2$

$$= \text{Total radiator weight} = 133,000 \text{ lb}$$

$$\text{Cylindrical area} \quad 29,100 \text{ ft}^2$$

$$\text{Conical area} \quad \frac{8,150 \text{ ft}^2}{37,250 \text{ ft}^2}$$

$$\frac{133,000}{37,250} = 3.57 \text{ lb/ft}^2$$

G. Compressor and Compressor Driver Weight

It is estimated that the specific weight of the compressors, in terms of pumping power, would be about 0.50 lb/kw. Therefore, allowing 1 Mw for compressor and prime mover losses (assuming 5 Mw actual pumping power):

Compressor weight allowance $0.50 \times 6000 \text{ kw} = 3000 \text{ lb}$

Although some savings in weight could be claimed by assuming that the driver cycles turbines are directly coupled to the gas cycle compressors, it will be assumed here that the compressors are motor driven. (This in fact simplifies the seals problem since the motors can be canned.) A fair estimate for the weight of the drive motors is about 1.0 lb/kw of pumping power. See Ref. 20 and driver cycle generator weight estimates (next Section). Therefore,

Drive motor allowance $1.0 \times 6000 = 6000 \text{ lb}$

H. Weight Totals—Fission-Electric Cell Reactor Gas Cycle

The total weight in pounds, and the total lb/kwe, for the reactor gas cycle are listed in Table 11.

Table 11. Weight totals, fission-electric reactor gas cycle

Item	Weight, lb	lb/kwe ^a
Reactor	76,800	3.08
Reflector	11,150	0.45
Pressure vessel	33,200	1.33
Reactor inlet manifold and feeder pipes	7,700	0.31
Radiator	133,000	5.3
Compressors	3,000	0.12
Drive motor	6,000	0.24
	<u>270,850</u>	<u>10.71</u>

^aBased on 25 Mw output.

VI. WEIGHT ESTIMATE—DRIVER-CYCLE COMPONENTS

A. Discussion

Calculations of the reactor physics parameters for the fission-electric cell space power reactor have indicated (Ref. 2), that a problem exists in the maintenance of criticality over a long period (10,000 hr). Excess reactivity must be built into the reactor. Increasing the fuel layer thickness severely reduces the efficiency of electrical conversion (Ref. 9 and Fig. 3). Short of developing a successful periodic or continuous refueling scheme (which has been suggested—see Ref. 2), some other means of adding fuel to the reactor, without decreasing efficiency, must be considered.

Ref. 2 shows that by adding fuel to the reactor in separate fuel modules (apart from the fission cells) reactor lifetimes on the order of 10,000 hr might be possible without increasing the fuel layer thickness. In effect, the non-fission-electric cell fuel modules act as separate sources of neutrons which "drive" the partially depleted fission-electric cells. Ref. 2 also shows that the driver power density would probably be many times the fission-electric cell power density, perhaps by as much as a factor of 20. This high power density suggests that the driver modules be cooled by a liquid metal. Typical

power density ranges for reactors utilizing various coolants are:

Gas coolants	1 Mw/ft ³
Pressurized water	3.5 Mw/ft ³
Liquid metals	3 – 30 Mw/ft ³

If it were not for the prospect of high power densities, it would be logical to remove the heat energy from the driver fuel modules with the same gas used to cool the fission-electric cells. A portion of the total heat energy could then be converted to electrical energy to drive the compressors and provide auxiliary power by means of a Brayton cycle employing a turbo-alternator. Use of fission-electric cell electrical output to supply pumping and auxiliary power is not ruled out, but was not considered for the following reasons: 1) the high voltage power output from the fission-cell reactor is better suited to direct use in an electric propulsion device, 2) the low conversion efficiencies to be expected from fission-electric cells make it desirable to use all of the available high voltage power available for propulsion, and 3) power converters of some kind would probably be required to reduce the voltage.

Assuming for the time being that it is feasible to have a gas coolant for the fission-electric cells, and a liquid metal coolant for the driver modules, one is then left with the choice of one or the other for consideration as the working fluid in a thermodynamic cycle to supply pumping and auxiliary power.

From Section II it is clear that about 6 Mw of electrical power should be sufficient to drive the compressors for the gas cycle. If it is assumed that 3 Mw of electrical power would be sufficient for all other spacecraft requirements, then for a conversion efficiency of 15%, a heat source of about 60 Mwt would supply the necessary auxiliary power. The total thermal power of the driver modules for a 500-Mw, 10-ft diameter fission-electric cell core has not yet been determined. However, it is estimated to be about the right magnitude to supply the auxiliary and pumping power, and for this reason weight estimates for a typical liquid metal vapor cycle are factored into the weight estimates of the preceding Section, for the gas cycle components, to obtain an overall estimate of the specific weight for such a plant.

A potassium vapor cycle seems to be a promising contender in the area of lightweight liquid metal vapor space power plant. For purposes of this weight estimate it will be assumed to be a logical choice for the driver working fluid.

B. Driver Cycle Weight Estimates — Potassium Vapor Cycle

1. ORNL Drawings

ORNL-LR-DWG 59803¹⁸ shows that for an effective radiator temperature of 1500°R a potassium system should produce a radiator weight of 3 lb/kw of electrical output, with no allowance for manifolds, meteoroid protection, or structure.

As shown in ORNL-LR-DWG 59810,¹⁹ the manifold specific weight should be proportional to the square root of the power system electrical output, varying from about 2 lb/kw at 1.5 Mwe to 5 lb/kw at 8 Mwe for a radiator temperature of 1500°R. It is assumed that the driver plant would be comprised of multiple and independent loops both for redundancy and to keep the manifold

¹⁸ORNL-LR-DWG 59803, Radiator Specific Weight as a Function of Mean Effective Radiator Temperature for a Stainless Steel Surface Having a Thickness of 0.036 in., an Emissivity of 0.90, and No Allowance for Manifolds or Structure.

¹⁹ORNL-LR-DWG 59810, Manifold Specific Weight as a Function of Electrical Power Output for Operation with Rubidium.

weight down to a minimum. A convenient division would be to assume four 1.5 Mwe loops to supply the pumping power and two 1.5 Mwe loops to supply the auxiliary power for a total of six loops and 9 Mwe. The radiator weight allowance would then be 2 lb/kw.

ORNL-LR-DWG 59828²⁰ indicates a radiator surface area for a 1 Mwe potassium cycle with 1500°R radiator temperature of 3,870 ft² or 3.87 ft²/kw. It is interesting to note that the surface area of the auxiliary radiator would then be $3,870 \times 9 \text{ Mwe} = 34,800 \text{ ft}^2$, for approximately 60 Mw heat dissipation. This is about the size of the high temperature gas cycle radiator which would service an electrical output of 25 to 50 Mwe and dissipate almost 500 Mw of waste heat.

According to ORNL-LR-DWG's 59802,²¹ 59809,²² and 59830,²³ if the peak cycle temperature were increased from 2000°R to 2500°R and the radiator temperature from 1500°R to 1700°R the radiator size could be reduced by about $\frac{1}{3}$ to 23,200 ft² with a reduction in specific weight of from 3 lb/kw to 2.0 lb/kw for the radiator surface, and from 2.0 to 0.2 lb/kw for the manifolds. The total radiator specific weight, not including meteoroid protection or radiator structure, would then be reduced from 5 lb/kw to 2.2 lb/kw. 1700°R is about the optimum radiator temperature for a peak cycle temperature of 2500°R.²⁴

2. Reactor

Less than 4% (30 ft³) of the total core volume would probably be required for the driver modules. It is not likely that the density of these modules would exceed 150 lb/ft³, so that the driver portion of the core should weigh less than $4500 \text{ lb} \div 8000 \text{ kw} = 0.56 \text{ lb/kw}$.

²⁰ORNL-LR-DWG 59828, Effects of Design Power Output on the Estimated Specific Weight of Potassium-Vapor-Cycle Power Plants Having a Turbine Inlet Temperature of 1540°F and a Condenser Inlet Temperature of 1040°F.

²¹ORNL-LR-DWG 59802, Radiator Area in Square Feet per Kilowatt of Heat Rejected and Radiator Specific Weight in Pounds per Kilowatt of Electrical Output for a Stainless Steel Surface Having a Thickness of 0.036 in. and an Emissivity of 0.90 Radiating to Space.

²²ORNL-LR-DWG 59809, Manifold Specific Weight as a Function of Electrical Power Output for Operation with Potassium.

²³ORNL-LR-DWG 59830, Effects of Design Power Output on the Estimated Specific Weight of Major Components of Potassium-Vapor-Cycle Power Plants Having a Turbine Inlet Temperature of 2040°F and a Condenser Inlet Temperature of 1240°F.

²⁴I.e., a higher radiator temperature would reduce cycle efficiency and require a larger radiator for the same power output.

3. Turbines and Pumps

It will be assumed that the potassium vapor turbines would contribute about²⁵ 0.1 lb/kw, or 900 lb. The fuel pumps will be assumed to contribute about half this amount or 0.05 lb/kw.

4. Generator

ORNL-LR-DWG 59818²⁶ summarizes various Air Force applications of alternators and shows a figure of 1.5 lb/kw for alternators with power outputs of 100 kw or greater. A recent study, Ref. (20), shows that generator specific weights of 0.5 lb/kw could be expected for space electric power generators for the power outputs of interest here.

The three best 1 Mw designs suggested by Ref. 20, Vol. 2, p. 24, are:

v	cps	rpm	Cool- ant	Wt, lb	Effi- ciency
500	2000	24,000	500°F	458	95.2%
1500	2000	24,000	500°F	463	95.4%
2140	2000	24,000	500°F	504	94.9%

Other possibilities at higher coolant temperatures²⁷ include:

v	cps	rpm	Cool- ant	Wt, lb	Effi- ciency
2140	2000	15,000	800°F	627	94.1%
2140	2000	6,000	1100°F	1678	92.4%

²⁵This should be compared with the specific weight of the turbine section of a typical turboprop aircraft engine: 0.03 lb/kw.

²⁶ORNL-LR-DWG 59818, Generator Specific Weight as a Function of Power Output.

²⁷As coolant temperature is increased, the rpm goes down and the weight increases. This is due to a maximum allowable rotor stress limitation.

The best 2 Mw designs are (Ref. 20, Vol. 2, p. 40):

v	cps	rpm	Cool- ant	Wt, lb	Effi- ciency
1000	2000	15,000	500°F	967	95.8%
1500	2000	15,000	500°F	988	95.3%
100	2000	20,000	500°F	1009	95.6%

Other possible 2 Mw designs include:

v	cps	rpm	Cool- ant	Wt, lb	Effi- ciency
1500	2000	10,000	800°F	1872	95.0%
1500	2000	4,000	1100°F	6247	90.2%

The generators of interest here would lie between 0.458 lb/kw and 1.678 lb/kw. A specific weight of 1.0 lb/kw will be assumed.

5. Miscellaneous Weight Items

A specific weight contribution of 2.5 lb/kw will be assumed for the potassium inventory and 2.5 lb/kw for connecting pipe, support structure, etc., for a total miscellaneous specific weight of 5.0 lb/kw.

6. Weight Totals — Driver Plant

Driver plant weight totals, at two different temperatures, are listed in Table 12.

Table 12. Weight totals, driver plant

Item	Radiator temperature	
	1500°R	1700°R
Radiator surface	3.0 lb/kw ^a	2.0 ^b lb/kw ^a
Radiator manifold	2.0	0.2
Driver core	0.56	0.56
Turbines and pumps	0.15	0.15
Generators	1.0	1.0
Miscellaneous	5.0	5.0
	11.71	8.91

^aBased on power output of the driver cycle. This is roughly the optimum radiator temperature for a peak cycle temperature of 2500°R, i.e., a higher radiator temperature would reduce cycle efficiency and require a larger radiator for the same power output.

^bEstimate 4.4 lb/kwe with meteoroid protection.

VII. WEIGHT SUMMARY

A. Weight Summary for 5% Conversion Efficiency

In Section V, the total specific weight for the gas cycle components was estimated at 10.7 lb/kw for 5% conversion efficiency (25 Mwe). And in Section VI, the total specific weight of the driver cycle components was estimated at 8.9 lb/kwe for 9000 kwe output and a radiator temperature of 1700°R.

The specific weight can now be calculated for the total plant. This is without shielding or meteoroid protection—however, as pointed out in a previous section, the gas radiator tubes may already be thick enough so as not to require meteoroid protection. At 5% conversion efficiency:

$$\begin{aligned}\text{Specific wt} &= \frac{10.7 \times 25,000 \text{ kw} + 8.9 \times 9,000}{25,000 + 3,000} \\ &= 12.4 \text{ lb/kw}\end{aligned}$$

With meteoroid protection, the potassium radiator specific weight could easily double: 4.4 lb/kw instead of 2.2 lb/kw. This would mean a driver specific weight of 11.1 lb/kw, instead of 8.9 lb/kw, and an overall specific weight of 13.1 lb/kw.

It is interesting to compare the estimated weights of the gas cycle (Table 11) with the estimated weights for the driver cycle (Table 12) and to compare radiator statistics (Table 13).

Even for a fission-electric conversion efficiency of only 5% the radiator specific area of 2.58 ft²/kwe for the driver cycle is almost twice that for the gas cycle radiator. The

specific area based on thermal capacity is almost five times as great for the driver cycle.²⁸

The higher area density for the gas cycle radiator can be attributed to the assumption that some use of high density refractory metal alloys would be required to cope with the high gas temperature.

B. Effect of Improved Fission-Electric Cell Conversion Efficiency

If the conversion efficiency of the fission-electric reactor were to be 10% instead of 5%, then a reactor of roughly the same size and thermal rating as analyzed in this report would be capable of producing 50 Mwe and the specific weights for the gas cycle in Table 13 would be halved, and the total plant specific weight would be:

$$\frac{5.25 \times 50,000 + 11.1 \times 9,000}{50,000 + 3,000} = 6.93 \text{ lb/kwe}$$

If, instead of converting improved fission-electric cell efficiency to higher power outputs, the original power goal of 25 Mwe is retained, then for 10% conversion efficiency the gas cycled weights and gas radiator statistics of Table 13 could be roughly cut in half for a total plant weight of about 235,000 lb. This is approximately the quoted earth orbit payload capacity of the *Saturn V* booster. The gas radiator size would be about 18,600 ft², which is equivalent to a cylinder 60 ft in diameter × 90 ft in length, and it seems possible that a plant with this

²⁸This is consistent with the ratio of effective radiator temperatures to the fourth power, i.e., (2500/1700)⁴ = 4.7.

Table 13. Comparison, gas cycle vs driver cycle

Item	Gas cycle ($\eta = 5\%$) 500 Mwt; 25 Mwe		Driver cycle ($\eta = 15\%$) 60 Mwt; 9 Mwe	
Reactor	87,950 lb ÷ 25,000 = 3.53 lb/kw		5,000 lb ÷ 9,000 = 0.56 lb/kw	
Radiator	133,000	5.3	29,600	4.4
Other	49,900	1.88	55,400	6.15
	270,850 lb	10.71 lb/kw	100,000 lb	11.11 lb/kw
Radiator:				
Area	37,250 ft ²		23,200 ft ²	
Heat load	~500 Mwt		~60 Mwt	
ft ² /kwt	76		386	
ft ² /kwe	1.49		2.58	
lb/ft ²	3.57		1.71	

size radiator could be launched as a single package. Clearly, if the radiator were five times as large, as would be the case with a liquid metal vapor plant limited to a

peak cycle temperature of 2500°R , a single launch to get the entire plant into earth orbit would probably be out of the question.

VIII. CONCLUSIONS

Conclusions reached were that:

1. A gas cooled fission-electric cell reactor with only 5% efficiency and a maximum gas temperature of 4000°R , utilizing a more conventional liquid metal vapor cycle for pumping and auxiliary power, could be competitive *on a specific weight basis*, with space power plants which depend entirely upon liquid metal vapor Rankine cycle for power conversion and operate at a conversion efficiency of about 15%.
2. The 5% efficient fission-electric plant would be more attractive than the liquid metal vapor plant on the grounds that the fission-electric plant could be made significantly smaller in size. This is due to the potentially high operating temperature for gas, the absence of a temperature differential penalty in the fission-electric cell energy conversion principle, and, consequently, a smaller radiator by about a factor of two.
3. A gas cooled fission-electric reactor with 10% conversion efficiency and a maximum gas temperature of 4000°R , could be as little as one half the weight of a liquid metal vapor Rankine plant limited to a peak cycle temperature of 2500°R . Furthermore, the size envelope for such a plant could be as little as one-fifth the size envelope of the Rankine cycle plant. This advantage might permit fission-electric reactor plants as large as 25 Mwe to be put into earth orbit in a single launch.

APPENDIX

Reactor Pressure Drop

I. FORMULATION OF PROBLEM

For constant specific heat, molecular weight, and mass flow rate: (see Ref. 13, p. 249, and Table 8.2)

$$\frac{dp_o}{p_o} = -\frac{\gamma M^2}{2} \left(\frac{dT_o}{T_o} + 4f \frac{dx}{D} \right) \quad (\text{A-1})$$

By Reynolds analogy (Eq. 7)

$$\frac{dT_o}{T_w - T_o} = 2f \left(\frac{1}{P_r} \right)^{0.6} \frac{dx}{D}$$

Substituting:

$$\frac{dp_o}{p_o} = \frac{d(p_o/p_{o1})}{p_o/p_{o1}} = -\frac{\gamma M^2}{2} \left(4f \frac{L}{D} \right) \left[\frac{1}{2} \frac{T_w - T_o}{T_o} \left(\frac{1}{P_r} \right)^{0.6} + 1 \right] d \left(\frac{x}{L} \right) \quad (\text{A-2})$$

However: (from Ref. 13, p. 230 or Ref. 3, p. 7)

$$\frac{p_{o1}}{p_o} = \frac{M}{M_1} \left(\frac{T_{o1}}{T_o} \right)^{1/2} \left(\frac{1 + \frac{\gamma-1}{2} M_1^2}{1 + \frac{\gamma-1}{2} M^2} \right)^{\frac{\gamma+1}{2(\gamma-1)}} \quad (\text{A-3})$$

Hence

$$M^2 = \left(\frac{p_{o1}}{p_o} \right)^2 \frac{T_o}{T_{o1}} \left(\frac{1 + \frac{\gamma-1}{2} M^2}{1 + \frac{\gamma-1}{2} M_1^2} \right)^{\frac{\gamma+1}{\gamma-1}} M_1^2 \quad (\text{A-4})$$

Substituting Eq. (A-4) in Eq. (A-2):

$$-\left(\frac{p_o}{p_{o1}} \right) d \left(\frac{p_o}{p_{o1}} \right) = \frac{\gamma}{2} M_1^2 \left(\frac{1 + \frac{\gamma-1}{2} M^2}{1 + \frac{\gamma-1}{2} M_1^2} \right)^{\frac{\gamma+1}{\gamma-1}} \left(4f \frac{L}{D} \right) \frac{T_o}{T_{o1}} \left[\frac{1}{2} \frac{T_w - T_o}{T_o} \left(\frac{1}{P_r} \right)^{0.6} + 1 \right] d \left(\frac{x}{L} \right) \quad (\text{A-5})$$

By a binomial expansion:

$$\left(1 + \frac{\gamma-1}{2} M^2 \right)^{\frac{\gamma+1}{\gamma-1}} \approx \left(1 + \frac{\gamma+1}{2} M^2 \right) + \dots \quad (\text{A-6})$$

where the expression in brackets is practically constant for small M . Integrating Eq. (A-5) with the Mach No. expression taken as constant at its mean value:

$$-\int_1^{(p_{o2}/p_{o1})} \left(\frac{p_o}{p_{o1}} \right) d \left(\frac{p_o}{p_{o1}} \right) = \frac{\gamma}{2} M_1^2 \left(\frac{1 + \frac{\gamma-1}{2} M^2}{1 + \frac{\gamma-1}{2} M_1^2} \right)^{\frac{\gamma+1}{\gamma-1}} \left(4f \frac{L}{D} \int_0^1 \frac{T_o}{T_{o1}} \left[\frac{1}{2} \frac{T_w - T_o}{T_o} \left(\frac{1}{P_r} \right)^{0.6} + 1 \right] d \left(\frac{x}{L} \right) \right)_{mean} \quad (\text{A-7})$$

which yields:

$$1 - \left(\frac{p_{o2}}{p_{o1}}\right)^2 = (\gamma M_1^2) \cdot B_1 \cdot \mathcal{Q}_1 \left(4f \frac{L}{D}\right) \quad (\text{A-8})$$

where

$$B_1 = \left(\frac{1 + \frac{\gamma-1}{2} M^2}{1 + \frac{\gamma-1}{2} M_1^2} \right)^{\frac{\gamma+1}{\gamma-1}}_{\text{mean}} \quad (\text{A-9})$$

and

$$\mathcal{Q}_1 = \int_0^1 \frac{T_o}{T_{o1}} \left[\frac{1}{2} \frac{T_w - T_o}{T_o} \left(\frac{1}{P_r}\right)^{0.6} + 1 \right] d\left(\frac{x}{L}\right) \quad (\text{A-10})$$

where T_o and T_w are functions of x .

Alternatively, it may be desirable to specify p_{o2} and T_{o2} , in which case M_2 is determined for a given value of $G (= \rho V$; see Section III of this Appendix). G is determined by the known heat load for the tube and by the desired value of $T_{o2} - T_{o1}$ which must be specified. Eq. (A-3) can be written:

$$\frac{p_o}{p_{o2}} = \frac{M_2}{M} \left(\frac{T_o}{T_{o2}}\right)^{1/2} \left(\frac{1 + \frac{\gamma-1}{2} M^2}{1 + \frac{\gamma-1}{2} M_2^2} \right)^{\frac{\gamma+1}{2(\gamma-1)}} \quad (\text{A-11})$$

Eq. (A-2) can be written:

$$\frac{d(p_o/p_{o2})}{(p_o/p_{o2})} = -\frac{\gamma M^2}{2} \left(4f \frac{L}{D}\right) \left[\frac{1}{2} \frac{T_w - T_o}{T_o} \left(\frac{1}{P_r}\right)^{0.6} + 1 \right] d\left(\frac{x}{L}\right) \quad (\text{A-12})$$

and substituting for M^2 :

$$\begin{aligned} -\left(\frac{p_o}{p_{o2}}\right) d\left(\frac{p_o}{p_{o2}}\right) &= \frac{\gamma}{2} M_2^2 \left(\frac{1 + \frac{\gamma-1}{2} M^2}{1 + \frac{\gamma-1}{2} M_2^2} \right)^{\frac{\gamma+1}{\gamma-1}} \left(4f \frac{L}{D}\right) \frac{T_o}{T_{o2}} \left[\frac{1}{2} \frac{T_w - T_o}{T_o} \left(\frac{1}{P_r}\right)^{0.6} + 1 \right] d\left(\frac{x}{L}\right) \\ -\int_0^1 \left(\frac{p_o}{p_{o2}}\right) d\left(\frac{p_o}{p_{o2}}\right) &= \frac{\gamma}{2} M_2^2 \left(\frac{1 + \frac{\gamma-1}{2} M^2}{1 + \frac{\gamma-1}{2} M_2^2} \right)^{\frac{\gamma+1}{\gamma-1}}_{\text{mean}} \left(4f \frac{L}{D}\right) \int_0^1 \frac{T_o}{T_{o2}} \left[\frac{1}{2} \frac{T_w - T_o}{T_o} \left(\frac{1}{P_r}\right)^{0.6} + 1 \right] d\left(\frac{x}{L}\right) \end{aligned} \quad (\text{A-13})$$

which yields:

$$\left(\frac{p_{o1}}{p_{o2}}\right)^2 - 1 = (\gamma M_2^2) B_2 \mathcal{Q}_2 \left(4f \frac{L}{D}\right) \quad (\text{A-14})$$

where

$$B_2 = \left(\frac{1 + \frac{\gamma-1}{2} M^2}{1 + \frac{\gamma-1}{2} M_2^2} \right)^{\frac{\gamma+1}{\gamma-1}}_{\text{mean}} \quad (\text{A-15})$$

and

$$\mathcal{Q}_2 = \int_0^1 \frac{T_o}{T_{o2}} \left[\frac{1}{2} \frac{T_w - T_o}{T_o} \left(\frac{1}{P_r}\right)^{0.6} + 1 \right] d\left(\frac{x}{L}\right) \quad (\text{A-16})$$

II. EVALUATION OF \mathcal{Q}_1 AND \mathcal{Q}_2

$$\mathcal{Q}_1 - 1 = \frac{1}{T_{o1}} \left\{ \frac{1}{2} \left(\frac{1}{P_r} \right)^{0.6} \left[\int_0^1 (T_w - T_{o1}) d\left(\frac{x}{L}\right) - \int_0^1 (T_o - T_{o1}) d\left(\frac{x}{L}\right) \right] + \int_0^1 (T_o - T_{o1}) d\left(\frac{x}{L}\right) \right\}$$

$$(\mathcal{Q}_1 - 1) \frac{T_{o1}}{T_{o2} - T_{o1}} = \frac{1}{2} \left(\frac{1}{P_r} \right)^{0.6} \int_0^1 \left(\frac{T_w - T_{o1}}{T_{o2} - T_{o1}} \right) d\left(\frac{x}{L}\right) + \left(1 - \frac{1}{2} \frac{1}{P_r} \right)^{0.6} \int_0^1 \left(\frac{T_o - T_{o1}}{T_{o2} - T_{o1}} \right) d\left(\frac{x}{L}\right)$$

From Eq. (2):

$$\int_0^1 \left(\frac{T_o - T_{o1}}{T_{o2} - T_{o1}} \right) d\epsilon = \int_0^1 (3\epsilon^2 - 2\epsilon^3) d\epsilon = \left(\epsilon^3 - \frac{1}{2} \epsilon^4 \right) \Big|_0^1 = \frac{1}{2}$$

$$(\mathcal{Q}_1 - 1) \frac{T_{o1}}{T_{o2} - T_{o1}} = \frac{1}{2} \left\{ \left(\frac{1}{P_r} \right)^{0.6} \left[\int_0^1 \left(\frac{T_w - T_{o1}}{T_{o2} - T_{o1}} \right) d\epsilon - \frac{1}{2} \right] + 1 \right\} \quad (\text{A-17})$$

Using Eq. (9), $(T_w - T_{o1})/(T_{o2} - T_{o1})$ can be easily integrated for various values of $4f(L/D)(1/P_r)^{0.6}$:

$$\int_0^1 \frac{T_w - T_{o1}}{T_{o2} - T_{o1}} d\epsilon = \frac{1}{4f \frac{L}{D} \left(\frac{1}{P_r} \right)^{0.6}} \left[12 \int_0^1 (\epsilon - \epsilon^2) d\epsilon \right] + \int_0^1 (3\epsilon^2 - 2\epsilon^3) d\epsilon = \frac{2}{4f \frac{L}{D} \left(\frac{1}{P_r} \right)^{0.6}} + \frac{1}{2}$$

\mathcal{Q}_2 is evaluated in the same way, except that:

$$(\mathcal{Q}_2 - 1) \frac{T_{o2}}{T_{o2} - T_{o1}} = \frac{1}{2} \left\{ \left(\frac{1}{P_r} \right)^{0.6} \left[\int_0^1 \left(\frac{T_w - T_{o1}}{T_{o2} - T_{o1}} \right) d\epsilon - \frac{1}{2} \right] + 1 \right\} \quad (\text{A-18})$$

Table A-1 presents the results of evaluating the right hand sides of Eq. (A-17) and (A-18) above for specific values of the lumped parameter $4f(L/D)(1/P_r)^{0.6}$.

Table A-1. Evaluation of the parameters \mathcal{Q}_1 and \mathcal{Q}_2

$4f \frac{L}{D} \left(\frac{1}{P_r} \right)^{0.6}$	$\int_0^1 \frac{T_w - T_{o1}}{T_{o2} - T_{o1}} d\epsilon$	$(\mathcal{Q}_2 - 1) \frac{T_{o2}}{T_{o2} - T_{o1}}$ or $(\mathcal{Q}_1 - 1) \frac{T_{o1}}{T_{o2} - T_{o1}}$
48	0.5416	0.526
36	0.5555	0.535
24	0.5834	0.557
18	0.6110	0.569
16	0.6250	0.578
12	0.6665	0.604
9	0.772	0.639
8	0.750	0.657
6	0.834	0.709
4.5	0.944	0.778
4	1.000	0.813
3	1.166	0.916
1.5	1.832	1.333
0.60	3.835	2.085

III. EVALUATION OF B_2 AND p_{o1}

$$B_2 = \left(\frac{1 + \frac{\gamma-1}{2} M^2}{1 + \frac{\gamma-1}{2} M_2^2} \right)^{\frac{\gamma+1}{\gamma-1}} \approx \frac{1}{2} \left[\left(\frac{1 + \frac{\gamma-1}{2} M_1^2}{1 + \frac{\gamma-1}{2} M_2^2} \right)^{\frac{\gamma+1}{\gamma-1}} + 1 \right] \quad (\text{A-19})$$

From Eq. (A-11)

$$\left(\frac{1 + \frac{\gamma-1}{2} M_1^2}{1 + \frac{\gamma-1}{2} M_2^2} \right)^{\frac{\gamma+1}{\gamma-1}} = \frac{M_1^2}{M_2^2} \left(\frac{p_{o1}}{p_{o2}} \right)^2 \frac{T_{o2}}{T_{o1}} \quad (\text{A-20})$$

$$B_2 = \frac{1}{2} \left[1 + \left(\frac{p_{o1}}{p_{o2}} \right)^2 \frac{T_{o2}}{T_{o1}} \frac{M_1^2}{M_2^2} \right] \quad (\text{A-21})$$

B_2 can be calculated as follows:

Assume $B_2 = 1$ in Eq. (A-14 or -22), to obtain a first estimate of p_{o1}

$$\left(\frac{p_{o1}}{p_{o2}} \right)^2 - 1 = (\gamma M_2^2) B_2 \mathcal{Q}_2 \left(4f \frac{L}{D} \right) \quad (\text{A-22})$$

Since p_{o2} and T_{o2} are specified, M_2 (see Eq. 20) can be determined from the following:

$$\left. \begin{array}{l} T_2 \approx T_{o2} \\ p_2 \approx p_{o2} \end{array} \right\} \text{for low Mach Nos.}$$

$$M_2 = \frac{V_2}{(\gamma R T_2 g_c)^{1/2}} = \frac{G}{\rho_2 (R T_2 g_c)^{1/2}} = \frac{G}{p_2} \left(\frac{R T_2}{\gamma g_c} \right)^{1/2} \quad (\text{A-23})$$

\mathcal{Q}_2 is determined as shown in Section II of this Appendix. The value of M_1 corresponding to the estimated value of

p_{o1} is found from Eq. (A-3):

$$\left(\frac{p_{o1}}{p_{o2}} \right) \left(\frac{T_{o2}}{T_{o1}} \right)^{1/2} = \frac{M_2}{M_1} \left[\frac{1 + \frac{\gamma-1}{2} M_1^2}{1 + \frac{\gamma-1}{2} M_2^2} \right]^{\frac{\gamma+1}{2(\gamma-1)}} \quad (\text{A-24})$$

For convenience, values of

$$\frac{1}{M} \left[\frac{2 \left(1 + \frac{\gamma-1}{2} M^2 \right)}{\gamma-1} \right]^{\frac{\gamma+1}{2(\gamma-1)}}$$

are tabulated in Table B.2 of Ref. 13.

Here,

$$\left(\frac{p_{o1}}{p_{o2}} \right) \left(\frac{T_{o2}}{T_{o1}} \right)^{1/2} = \frac{\frac{1}{M_1} \left[\frac{2 \left(1 + \frac{\gamma-1}{2} M_1^2 \right)}{\gamma-1} \right]^{\frac{\gamma+1}{2(\gamma-1)}}}{\frac{1}{M_2} \left[\frac{2 \left(1 + \frac{\gamma-1}{2} M_2^2 \right)}{\gamma-1} \right]^{\frac{\gamma+1}{2(\gamma-1)}}} \quad (\text{A-25})$$

An improved value of B_2 is then calculated from Eq. (A-19) substituted into Eq. (A-22) and the process is repeated until convergence is obtained (usually in only one or two steps). The final values of p_{o1} is then found from Eq. (A-22).

NOMENCLATURE

A	area	Q	heat load (Btu/hr or Btu/hr-ft)
B, \mathcal{O}	dimensionless parameters	Q_I	pumping power (usually expressed in Mw)
c	velocity of sound in the medium $c^2 = (\gamma p g_c / \rho) = \gamma R T g_c$	q	heat flux (Btu/hr—unit of area)
c_p, c_v	coolant specific heat at constant pressure, volume (Btu/lbm — °R)	R	gas constant $R = 772$ ft-lbf/lbm — °R for H_2 $R = 386$ ft-lbf/lbm — °R for He
D	diameter	S	thermal stress
D_R	radiator diameter	T_a	anode surface temperature
E	modulus of elasticity (lb/in. ²)	T_c	cathode surface temperature
\mathcal{E}	emissivity—radiant heat transfer surface	T_{o1}	stagnation temperature-channel inlet
F	radiation heat transfer shape factors	T_{o2}	stagnation temperature-channel outlet
$F(T_s)$	surface temperature parameter; see Eq. (42)	T_s	radiator tube surface temperature
f	fanning friction factor defined by $T_w = f \rho (V^2 / 2 g_c)$ (f dimensionless) where T_w = shear stress at wall	T_w	tube wall temperature, inside surface
G	$G = \rho V$ = mass flux (lbm/ft ² -hr)	t	temperature or wall thickness
g_c	gravitational constant $g_c = 32.2$ (lbm-ft/lbf-sec ²)	V	fluid velocity averaged over channel cross section (ft/hr)
h	surface heat transfer coefficient (Btu/hr-ft ² -°R)	W	mass flow rate (lbm/hr)
$J_0(r)$	Bessel function	α	thermal expansion coefficient (in./in.-°R)
k	conductivity (Btu/hr-ft-°R)	γ	ratio of specific heats $\gamma = c_p / c_v$
L	length	Δh	enthalpy change (Btu/lbm)
L_R	radiator length	Δp	pressure difference
M	Mach No., $M = V/c$	ϵ	dimensionless distance parameter, $\epsilon = x/L$
n, N	number of tubes	μ	coolant viscosity (lbm/hr-ft)
P_r	Prandtl No. $P_r = c_p \mu / k$ (dimensionless)	ν	Poisson's ratio
p_{o1}	stagnation pressure-channel inlet	ρ	density (lbm/ft ³)
p_{o2}	stagnation pressure-channel outlet	ρV	mass flux (lbm/ft ² -sec)
		σ_H	hoop stress

REFERENCES

1. Krieve, W. F., Heindl, C. J., and Meghreblian, R. V., "Fission Fragment Conversion Reactors for Space," *Nucleonics*, p. 80, April 1963.
2. Shapiro, J. L., *The Two Region Fission-Electric Cell Reactor*, Technical Report No. 32-685, Jet Propulsion Laboratory, Pasadena, Calif.

REFERENCES (Cont'd)

3. Bartz, D. R., *Analysis of the Thermal Design Limitations of the Solid-Core Reactors for Nuclear Propulsion*, Technical Report No. 32-217, Jet Propulsion Laboratory, Pasadena, Calif., November 15, 1962.
4. *Aerospace Engineering*, Vol. 22, No. 1, January 1963 (High Temperature Issue).
5. Taylor, Maynard F., "Local Heat Transfer Measurements for Forced Convection of Hydrogen and Helium at Surface Temperatures up to 5600°R," *Proceedings of the 1963 Heat Transfer and Fluid Mechanics Institute*, Lewis Research Center, NASA.
6. Evvards, J. C., "How Much Future for Electric Propulsion?" *Astronautics and Aerospace Engineering*, p. 92, August 1963.
7. Grey, J., and Williams, R. M., "A Re-Examination of Gas Cycle Nuclear-Electric Space Power Plants," *AIAA Electric Propulsion Conference*, Princeton University, Princeton, N. J., March 1963.
8. "Redesigned SNAP-8 To Be Heavier But More Reliable," *Nucleonics*, p. 79, July 1963.
9. Heindl, C. J., *Efficiency of Fission Electric Cells*, Technical Report No. 32-105, Jet Propulsion Laboratory, Pasadena, Calif., May 25, 1961.
10. Stone, R., and Combs, M., "Design of a Heat Rejection System for the SNAP 2 Space Nuclear Power System," *ASME paper 60-WA-237*, Winter Annual Meeting, New York, November 27-December 2, 1960.
11. *The ORNL Gas-Cooled Reactor*, ORNL-2500, Oak Ridge National Laboratory, Oak Ridge, Tenn., April 1, 1958.
12. Bussard, R. W., and DeLauer, R. D., *Nuclear Rocket Propulsion*, McGraw-Hill Book Company, New York, 1958.
13. Shapiro, Ascher H., *The Dynamics and Thermodynamics of Compressible Fluid Flow*, Vol. 1 and 2, The Ronald Press Co., New York, 1953.
14. Carslaw, H. S., and Jaeger, J. C., *Conduction of Heat in Solids*, Clarendon Press, Oxford, England, 1959.
15. Timoshenko, Stephen, and Goodier, S. N., *Theory of Elasticity*, 2nd Edition, McGraw-Hill Book Company, New York, 1951.
16. Kreith, Frank, *Principles of Heat Transfer*, International Textbook Co., Scranton, Pa., 1960.
17. McAdams, W. H., *Heat Transmission*, 3rd Edition, McGraw-Hill Book Company, New York, 1954.
18. Zucrow, H. J., *Aircraft and Missile Propulsion*, Vol. 1, Wiley & Sons, Inc., New York, 1958.
19. "Engineering," *Reactor Handbook*, Vol. 2, Engineering, p. 477, Technical Information Service, U. S. Atomic Energy Commission, Declassified Edition, May 1955.
20. *Space Electric Power Systems Study*, Final Report, Vol. 1-4, Westinghouse Electric Corporation, Aerospace Electrical Division, Lima, Ohio, November 1961-December 1962.

BIBLIOGRAPHY

Heindl, C. J., *Comparison of Fission Electric Cell Geometries*, Technical Report No. 32-101, Jet Propulsion Laboratory, Pasadena, Calif., September 1, 1961.

Jakob, Max, *Heat Transfer*, John Wiley & Sons, Inc., New York, 1958.

Safonov, George, *Direct Conversion of Fission to Electric Energy in Low Temperature Reactors*, Rand Corporation Report, RM-1870, January 8, 1957.

Vennard, John K., *Elementary Fluid Mechanics*, John Wiley & Sons, Inc., New York, 1961.

The Permeation of Hydrogen Through Constructional Materials, Report ER 4776, Thompson-Ramo-Wooldridge, Inc., Cleveland, Ohio, June 1962.

ACKNOWLEDGMENT

The author wishes to express his thanks to Drs. C. J. Heindl, J. L. Shapiro and H. J. Stumpf for many useful suggestions and comments. He also wishes to acknowledge the most helpful assistance of Lois I. Bush for programming and running the fluid mechanics analysis for the reactor portion of this study, and of Gail Keller and Sayuri Harami, for carrying out the thermal and fluid mechanics computations on the radiator portion.